Shifting baseline in macroecology? Unraveling the influence of human impact on mammalian body mass

Article

Accepted Version

Santini, L., González-Suárez, M., Rondinini, C. and Di Marco, M. (2017) Shifting baseline in macroecology? Unraveling the influence of human impact on mammalian body mass. Diversity and Distributions, 23 (6). pp. 640-649. ISSN 1472-4642 doi: https://doi.org/10.1111/ddi.12555 Available at http://centaur.reading.ac.uk/69201/

To link to this article DOI: http://dx.doi.org/10.1111/ddi.12555

Publisher: Wiley

Article type: Original article

Title: Shifting baseline in macroecology? Unraveling the influence of human impact on mammalian body mass

Running head: Human impact on mammalian body mass patterns

Luca Santini[1,2*], Manuela González-Suárez[3,4], Carlo Rondinini[2], Moreno Di Marco[5,6]

[1] Department of Environmental Science, Radboud University, P.O. Box 9010, NL-6500 GL, Nijmegen, The Netherlands

[2] Global Mammal Assessment program, Department of Biology and Biotechnologies, Sapienza Università di Roma, Viale dell'Università 32, 00185 Rome, Italy

[3] Department of Conservation Biology, Estación Biológica de Doñana - CSIC, 41092 Seville, Spain.

[4] Ecology and Evolutionary Biology, School of Biological Sciences, University of Reading, Whiteknights, Reading, Berkshire, RG6 6AS, UK

[5] ARC Centre of Excellence for Environmental Decision, Centre for Biodiversity and Conservation Science, The University of Queensland, St Lucia, QLD 4072 (Brisbane, Australia).

[6] School of Earth and Environmental Sciences, The University of Queensland, St Lucia, QLD 4072 (Brisbane, Australia).

Corresponding author: Luca Santini, luca.santini.eco@gmail.com

Abstract

Aim Human activities have led to hundreds of species extinctions and have narrowed the distribution of many of the remaining species. These changes influence our understanding of global macroecological patterns, but their effects have been rarely explored. One of these patterns, the Bergmann’s rule, has been largely investigated in macroecology, but often under the assumption that observed patterns reflect “natural” processes. We assessed the extent to which humans have re-shaped the observable patterns of body mass distribution in terrestrial mammals, and how this has altered the macroecological baseline.

Location Global

Methods Using a comprehensive set of ecological, climatic, and anthropogenic variables we tested several alternative hypotheses to explain the body mass pattern observed in terrestrial mammals assemblages at a 1-degree resolution. We then explored how model predictions and the Bergmann’s latitudinal pattern are affected by the inclusion of human impact variables, and identified areas where predicted body mass differs from the expected due to human impact.

Results Our model suggests that median and maximum body mass predicted in grid cells would be higher, and skewness in local mass distributions reduced, if human impacts were minimal, especially in areas that are highly accessible to humans and where natural land cover has been converted for human activities.

Main conclusions Our study provides evidence of the pervasive effects of anthropogenic impact on nature, and shows human-induced distortion of global macroecological patterns. This extends the notion of “shifting baseline”, suggesting that when the first macroecological investigations started, our understanding of global geographic patterns was based on a situation which was already compromised. While in the short term human impact is causing species decline and extinction, in the long term it is causing a broad re-shaping of animal communities with yet unpredicted ecological implications.

Keywords: Accessibility, Bergmann’s rule, Defaunation, Extinction, Human impact, Land use change, Terrestrial mammals, Vulnerability

1. Introduction

The current human impact on nature is pervasive, and land-use change has considerably reshaped the Earth's surface and disrupted natural dynamics (Newbold et al., 2016). Hundreds of vertebrate species have become extinct in the last centuries, and many of the remaining species have shown declines in abundance and contractions in distribution (Dirzo et al., 2014). The extent of these changes has led to an alteration of natural macroecological patterns (Murray & Dickman, 2000; Diniz-Filho et al., 2009; Di Marco & Santini, 2015a; Faurby & Svenning, 2015; Torres-Romero & Olalla-Tárraga, 2015), to the point that current patterns may have become a poor reflection of the original biogeographical drivers (Di Marco & Santini, 2015a; but see Olalla-Tárraga et al., 2015; Di Marco & Santini, 2015b).

Since Bergmann's prediction that animal body mass increased with latitude (Bergmann, 1847), the intra- and interspecific spatial distribution of body mass has been one of the most investigated global macroecological patterns (Blackburn et al., 1999; Meiri, 2011). However, after more than 160 years, the so-called Bergmann's rule is still under debate (Blackburn et al., 1999; Meiri, 2011) with a number of alternative explanations proposed. The original explanation by Bergmann has taken the name of "heat conservation hypothesis" and predicts that organisms in colder areas tend to be larger because the reduction in their surface/volume ratio that results from increased size limits heat dissipation (Bergmann, 1847). Size may also affect the evaporative cooling rate in moist and warm climate, favouring small–bodied species (the "heat dissipation hypothesis"; Brown & Lee, 1969; James, 1970; Speakman & Król, 2010). A larger body mass can reduce the risk of starvation as proposed by the "starvation resistance hypothesis", allowing a species to cope with the seasonal shortage of resources that occur in higher latitudes (Calder, 1984; Lindstedt & Boyce, 1985; Dunbrack & Ramsay, 1993). Larger species also disperse longer distances, which could have influenced their ability to re-colonize high latitudes after the Pleistocene ice-sheet retreat, as proposed in the “dispersal hypothesis” (Blackburn & Hawkins, 2004). Finally, the “resource-rule” suggests that the pattern may arise from the latitudinal pattern of resources availability reflecting gradients of climate and biological competition (McNab, 2010). No hypothesis alone is able to explain the observed patterns for all taxa, and several non-exclusive explanations have found empirical support (Rodríguez et al., 2006; Rodriguez et al., 2008; Diniz-Filho et al., 2009; Olson et al., 2009). Interestingly, all proposed mechanisms assume that observable patterns are determined by “natural” environmental conditions, largely disregarding past and present human impacts.

Investigation of the distribution of mammalian body mass and how humans have changed observable patterns is of direct relevance for conservation assessments. Species vulnerability to extinction is generally positively correlated with body mass. Large species are at much higher risk than small ones (Purvis et al., 2000; Cardillo et al., 2005; Di Marco et al., 2014a) and have a higher probability of facing an increase in risk over time (Di Marco et al., 2015). This is because large species tend to live at low densities (Damuth, 1981) and have slow rates of population growth as compared to small species (Fenchel, 1974; Johnson, 2002). In addition, large-bodied mammals have been largely persecuted by humans for meat (Milner-Gulland & Bennet, 2003; Corlett, 2007), to reduce conflicts with human activities (Woodroffe, 2000), or for trophy hunting (Allendorf & Hard, 2009). Scattered evidence suggests that the spatial patterns in body mass that we observe today have been influenced by past human impact, including human-induced megafauna extinctions in the Pleistocene (Smith & Lyons, 2011; Morales-Castilla et al., 2012), and large fauna extinctions from agricultural development in historical times (Fritz et al., 2009). More recent extinctions, as well as contractions of species' geographic ranges (Diniz-Filho et al., 2009; Di Marco & Santini, 2015a; Faurby & Svenning, 2015) may have also played a central role in re-shaping global species assemblages (Ripple & Van Valkenburgh, 2010). Indeed, there are only a few areas worldwide left where the megafauna can be considered intact (Morrison et al., 2007; Faurby & Svenning, 2015). It has also been argued that the skewness of the distribution of mammal body mass in the Holocene has been exacerbated due to the extinction large species in the Pleistocene (Lyons et al., 2004; Smith & Lyons, 2011). Simulations have also suggested that the non-random extinction of large-bodied species has likely contributed to the observed skewness in body mass distribution (Maurer et al., 1992). Characterizing human impacts on body size distributions can help us identifying altered mammalian assemblages and more pristine and potentially sensitive communities.

Here we investigate how ecological, climatic, and anthropogenic variables predict the current distribution of body mass in mammal species assemblages using a 1-degree grid covering the world's land surface. We then predict how body mass values would change if the effects of human impact were minimal and whether the relationship between latitude and body mass (Bergmann's rule) has been distorted by human impact as has previously been argued (Faurby & Araújo, 2016). We hypothesize that mammal species assemblages have overall reduced body size in proportion to the intensity and duration of human impacts. We also hypothesize that the skewness in body mass distribution has been increased by the loss of large species. Furthermore, because human impacts are not homogenously distributed across the planet, we expect a weaker relationship between latitude and body mass in the Northern hemisphere, where impacts are predominant.

2. Methods

2.1. Spatial grid of body mass distribution

We analysed data for 5,242 terrestrial mammal species for which distribution and body mass information were available (~98% of all terrestrial mammals). We used the geographic range polygons published by the Red List of the International Union for Conservation of Nature to represent species distributions (IUCN, 2015), and obtained body mass data from Pacifici et al. (2013) which is largely based on the PanTHERIA dataset (Jones et al., 2009). We analysed the geographical pattern of body mass at the assemblage level (Olalla-Tárraga et al., 2010), and used a 1-degree resolution grid (in lat-long) covering the world's lands whereby species were assigned to cells which were entirely or partly overlapping with their ranges. Assemblage level approaches are ideal to investigate the geographical pattern of the Bergmann' rule because they allow to directly assess the underlying environmental structure. With alternative cross-species approaches this structure would be severely limited because environmental gradients are reduced to a single point in the geographical space (Olalla-Tárraga et al., 2010). For each grid cell, we then calculated the median, maximum and skewness of untransformed body mass values (Fig. 1; Meiri & Thomas, 2007). We excluded from analyses cells with ≤5 species. The maximum was expressed as the 90th percentile of the statistical distribution of body mass values in order to avoid capturing outliers (Blackburn & Hawkins, 2004) , and it was only calculated for cells with >10 species.

2.2. Environmental and human impact variables

We considered 12 potential environmental predictors of species body mass following previous macroecological research on body mass distribution in endotherms. We represented climatic conditions considering: mean annual temperature, mean temperature of the coldest quarter, mean temperature of the warmest quarter, mean annual precipitation, mean precipitation of the driest quarter, mean precipitation of the wettest quarter, and actual evapotranspiration (AET). Temperature is directly linked with the heat conservation hypothesis, whereas precipitation and AET are linked to the heat dissipation hypothesis (Blackburn & Hawkins, 2004; Rodríguez et al., 2006; Rodriguez et al., 2008; Diniz-Filho et al., 2009; Olson et al., 2009). Temperature and precipitation variables were downloaded from WorldClim (Hijmans et al., 2005) for the period 1950-2000. AET and PET were downloaded from http://www.grid.unep.ch/data/summary.php?dataid=GNV183 for the period 1920-1980. Additionally as a measure of mesoscale climatic variation and environmental heterogeneity within cells (Blackburn & Hawkins, 2004; Rodríguez et al., 2006; Rodriguez et al., 2008; Diniz-Filho et al., 2009; Olson et al., 2009) we used the range in elevation calculated from the global relief model ETOPO1 (Amante & Eakins, 2009). We represented primary productivity using the Normalized Difference of Vegetation Index (NDVI; http://neo.sci.gsfc.nasa.gov/view.php?datasetId=MOD13A2_M_NDVI). We used monthly estimates from 2000 to 2012 to calculate annual mean productivity and the coefficient of variation in NDVI within year as a proxy of seasonality in primary productivity (Blackburn & Hawkins, 2004; Rodríguez et al., 2006; Rodriguez et al., 2008; Diniz-Filho et al., 2009; Olson et al., 2009). The periods represented by these variables differ because data were not available for the same periods. To account for historical processes that could influence body mass distribution we estimated "time since last glacial retreat" following Rodríguez et al. (2006). Finally, body mass values in an area might be influenced by species richness (Meiri & Thomas, 2007; Olson et al., 2009), hence we controlled for this potential influence by including taxonomic Order richness as a predictor. We used Order richness because it is more robust to recent local extinctions than species richness, and thus more adequate when making predictions that assumed no human impacts (see below). We acknowledge that this approach has potential limitations for smaller orders, characterised by few large-bodied species (e.g. Proboscidata, Perissodactyla), yet, for most groups that include many of the largest mammals (e.g., Carnivora and Cetartiodactyla) it would be more robust.

We additionally considered four variables representing levels of human impact on natural environments: human population density (ind/ha) in the year 2000 (CIESIN & CIAT, 2005); percentage of agricultural land calculated from Globcover satellite images at year 2009 (IONIA, 2009); accessibility, expressed as travel time (hours) from major cities (>50,000 people; Nelson, 2008); and history of land use, expressed as time from first human use, spanning from 0 (never used) to 8000 (first used in 6000 bc), derived from the KK10 model of historical land use intensity (Ellis et al., 2013). Following Ellis *et al*. (2013) we considered a cell as significantly used when the percentage of land classified as human use was >20%.

2.3. Statistical analyses

To avoid potential collinearity issues (see Table S1 in Supporting Information) in model fitting and to reduce model complexity, we performed a principal component analysis (PCA). Prior to perform the PCA, mean annual precipitation, mean precipitation of the wettest quarter, mean precipitation of the driest quarter, AET, range in elevation, order richness and NDVI seasonality were log10-transformed to reduce distribution skewness, and all variables were standardized to a mean of zero and a SD of one. To determine the number of components to retain we tested axes significance based on the broken-stick criterion (Legendre & Legendre, 1998). We selected the first two components that were significant and together explained 64.3% of the variance (Table S2-S3).

We then fitted and compared alternative models to predict either the median or maximum body mass values (log10-transformed to meet model assumptions) in each grid cell (Table 1). The null model included only the selected principal components reflecting environmental characteristics. Additional models were built by adding combinations of one or two human impact variables (Table 1). Some combinations of impact variables were not tested because of high correlation among variables (Pearson $r \geq 0.7$). All human impact variables were also log10-transformed to meet linearity assumptions in our models. Because large bodied species need large areas to form viable populations, body mass is also constrained by island size. In order to account for area constraints in body mass all models were also run including the factor “islands” to allow the intercept to adjust at different values. Islands were defined as all land masses smaller than an area threshold. We defined 4 thresholds: 25,000 km^2 (102 cells), 100,000 km^2 (231 cells), 500,000 km^2 (386 cells), and 7,500,000 km^2 (724 cells; ~ all lands smaller than Australia).

Each model was first fitted using ordinary least square regression (OLS) and we tested for spatial autocorrelation in the residuals using Moran Index. Because models’ residuals were always significantly autocorrelated (Table S4), we used spatial auto-regressive linear models (SAR) with a rook neighbourhood to compare proposed models and estimate coefficients. We used the function “errorsarlm” from the package "spdep" in R 3.0.3 (R Core Team, 2016). This spatial error model assumes that the autoregressive process is found only in the error term, and it has been found to perform better than OLS and other SAR models (Kissling & Carl, 2008). This approach removed most of the spatial autocorrelation in the residuals (Fig. S1).

Models were compared using Bayesian Information Criterion (BIC) weights (ω), indicating the relative weight of evidence of competitive models (Burnham & Anderson, 2002). We used BIC rather than the more commonly used Akaike Information Criterion (AIC) because it is more conservative in estimating differences between competitive models when sample size is high (n>15,000 in this study) and tends to select for simpler, more parsimonious models (Raffalovich et al., 2008). However, for comparison, we also report the results of model selection based on AIC in supporting material (Table S7). Following Burnham and Anderson (2002) we calculated predicted values based on a single model if clearly identified as best ($\omega > 0.9$) or using weighted estimates obtained by averaging predictions of all models weighted by ω. We calculated the variance explained by the models as pseudo-R^2, by taking the square of the correlation coefficient between the fitted values and the observed variable (R^2_{sp}), and the square of the correlation coefficient between the predicted values using the coefficients only (not the spatial part) and the observed variable (R^2_{nsp}). While the former indicate the variance explained by the fixed factor and the spatial autocorrelation combined, the latter indicate the variance explained by the fixed factors only. The model selection procedure described above was replicated using skewness in body mass as the response variable. Mammalian body mass distribution has been shown to be both phylogenetically and spatially autocorrelated at a global scale (Villalobos et al., 2016). However, phylogenetic relatedness in assemblage-level analyses is a substantially smaller problem than in cross-species analyses, and the method proposed to control for both spatial and phylogenetic autocorrelation in assemblage-level analyses (eigenvector regression) (Diniz-Filho et al., 1998, 2009) has been criticized (Adams & Church, 2011; Freckleton et al., 2011).

Using the SAR models, we then predicted mean and maximum body mass per grid under two scenarios of anthropogenic impact: observed impact and minimal impact. The first scenario corresponded to the fitted values from the best model (or a ω-weighted average prediction from all models if no single model was clearly supported). For the second scenario, we simulated minimal human impacts by assigning to each grid cell the lowest observed value of each human impact variable in the model, while retaining the environmental variable values, and recalculating its predicted mean and maximum body mass (as above by weighted average if no single model was clearly supported). To estimate the expected loss in median and maximum body mass, we then calculated the difference (delta) between the predictions under the two scenarios of human impact.

To assess whether Bergmann's rule is affected by human impact, we explored the relationship between latitude and predicted body mass for each scenario. To avoid longitudinal autocorrelation in these analyses, we treated longitudinal bands as random effects (1 degree of longitude) and then modelled these mass values as a function of latitude allowing for separate intercept and slope estimates for each scenario. We used the function "lme" from the package "nlme". Because the observed relationship between latitude and body mass is non-linear with an inflection around 20°N, we actually fitted three linear regression models: above 20° of latitude in the northern hemisphere, between 0° and 20°N, and southern hemisphere. All spatial analyses were performed using the package "raster" (Hijmans et al., 2005) and "maptools" (Lewin-Koh & Bivand, 2011) in R 3.0.3 (R Core Team, 2016).

2.4. Comparison with historical data

As a mean of cross-validation, we compared the results obtained with our approach based only on contemporary data with calculated differences in current vs. historical body mass distributions (Faurby & Araújo, 2016). We calculated historical mean and maximum body mass per cell using the historical ranges available from Faurby & Svenning (2015) following the same procedure described above for the current ranges (Fig. S2). Because our approach is likely to only capture relatively recent anthropogenic effects, we only retained species recognized by the IUCN in the historical dataset, which correspond to those persisting at least until 1,500 AD. Body mass estimates for extinct species were primarily obtained from Smith *et al.* (2003), and supplemented with data from publications on specific species (MacPhee & Grimaldi, 1996; Goodman et al., 2004; van Vuure, 2005; Faurby & Svenning, 2016). For extinct species for which no estimate was available we used the mean body mass from its congeners. We calculated the agreement between both estimates simplifying the change in body mass between current and historical species distribution to a binary response (predicted decrease in mass=1, no decrease or increase=0). This simplification allows measuring the agreement of the two models in terms of areas where large-bodied species have been lost, rather than an agreement in the exact values that was not expected *a priori* given the differences in the methodologies and in the group of species considered. To quantify the overall agreement we estimated the Area Under the Curve (AUC) of a Receiving Operating Characteristics curve that assesses the performance of a binary classifier comparing the true and false positive rates. We used historical changes as observed and changes predicted by our model as expected.

3. Results

3.1. Influence of anthropogenic impact on body mass distribution

The best models for median and maximum body mass (Table 1, Table S5) included one or two of the human impact variables considered. Travel time from major cities (a proxy of accessibility to humans) showed a positive relationship with median and maximum body mass, indicating that larger species tend to inhabit more inaccessible areas (Table 2; Table S6). Similarly, median body mass decreased with increasing time from first land use, indicating that larger mammals are found in more pristine areas. Maximum body mass was lower in islands than in mainland.

We found similar results for skewness in body mass distribution. For this variable no model was unequivocally supported ($\omega>0.9$). The three most supported models ($\omega>0.1$) included accessibility, percentage of agricultural area, time from first land use, and the factor island (Table 1; Table S5). Skewness increased with increasing percentage of agricultural areas and time from first land use, and decreased with increasing travel time from major cities. In islands skewness was lower (Table 1; Table S6). Qualitatively similar results were found using AIC for model selection (Table S7).

3.2. Alteration of body mass distribution pattern

The relationship between latitude and median body mass (Bergmann's rule) is negative in the northern hemisphere above 20°N and in the southern hemisphere, but positive between 0° and 20°N. Conversely, the relationship between latitude with maximum body mass was positive with latitude above 20°N and slightly positive in the southern hemisphere, and slightly negative between 0° and 20°N. The slopes decreased in the northern hemisphere above 20° with human impact for median and maximum body mass, increased between 0° and 20°, and decreased for the Southern hemisphere for both median and maximum body mass (Table 2; Fig. 2).

Comparing the best model predictions under the two scenarios, we estimated that under the minimal human impacts scenario we would expect an increase of 123.9 ± 37.4 g (mean ± SD) in median body mass and of 9.9 ± 2.4 kg in maximum body mass, corresponding to a relative increase of 22.4 ± 5.7 % and 25.6 ± 6.2 % respectively (Fig. 3). For mainlands, median and maximum body mass loss were particularly noticeable in United States, Southeastern Brazil, Europe, Sub-Saharan Africa, Central and South East Asia, and Southern east and west Australia. In general islands showed lower absolute losses, but similar relative values (Fig. 3).

3.3. Comparison with historical dataset

Our results were generally consistent with estimates based on current and historical data, although historical data suggested larger changes than our predictions in general, but negative changes in the Amazon basin and Australia (Fig. S3). We calculated AUC values of 0.51 and 0.71 for the mean and maximum body mass respectively indicating no and moderate agreement in change tendency.

4. Discussion

4.1. Alteration of body mass distribution pattern

Our results indicate that the present values of mammalian body mass are lower than those expected under “natural” environmental conditions alone. Current body mass distribution in terrestrial mammal assemblages appeared largely influenced by existing human impacts. In particular, high body mass values were associated with remote areas (those requiring longer travel times from major cities), lower human population density and with no or recent land conversion. Human population density and accessibility can be considered proxies of many human disturbance factors including over-exploitation from hunting and persecution (Nelson, 2008). Conversion to agriculture has direct effects on local extinctions, by replacing natural habitat with lands unsuitable to most species. Our analyses showed that both current and past conversion can be relevant. Importantly, models including descriptors of human impacts were more supported than the null models based only on “natural” conditions, indicating that anthropogenic effects must be considered when trying to understand current macroecological patterns.

Our results showed that the relationship between latitude and body mass, (Bergmann’s rule) has been altered during the “Anthropocene”. We observed a vertical shift in the relationship due to a widespread reduction in median and maximum body mass. Noticeably, the shape of the relationship did not conform well to the expectations derived from the Bergmann’s rule, and the slopes were altered by human impact at the three different latitudinal belts (>20° of latitude in the northern hemisphere, between 0° and 20°N, and southern hemisphere), which could reflect an unequal latitudinal intensity of human pressure. The presence of species with different sensibilities (Fritz et al., 2009) is also likely responsible for this observed difference. This result obtained through a statistical approach agrees with that obtained by Faurby & Araujo (2016) that looked at the comparison between current and historical ranges.

Under the minimal human impact scenario, the largest absolute increase of body mass was predicted in northern temperate areas, Sub-Saharian Africa and South-East Asia, whereas when expressed as relative increase it was more evenly distributed. These changes likely reflect distinct processes. The difference between expected and observed body mass might reflect the loss of megafauna that occurred during the late-Pleistocene and Holocene (Lister & Stuart, 2007; Barnosky & Lindsey, 2010; Woinarski et al., 2015). Yet, is likely that our model mostly capture more recent impacts. In northern temperate areas large species have disappeared in historical times, such as the auroch (*Bos primigenius*) and the tarpan (*Equus ferus ferus*), while others have largely contracted their ranges, especially ungulates and carnivores. Africa hosts the largest mammalian fauna today, although populations of African mammals have declined substantially in recent times due to human impacts (Craigie et al., 2010; Di Marco et al., 2014b), and many large species such as the African elephant (*Loxodonta africana*) or the white rhino (*Ceratotherium simum*) have suffered recent and severe range contractions (Ripple et al., 2014, 2015; IUCN, 2015). India and Southeast Asia have also experienced widespread range contractions and the loss of some large-bodied species recently due to the interactive effect of unsustainable hunting, habitat degradation, and more recently illegal wildlife trade (Sodhi et al., 2004; Corlett, 2007).

4.2. Potential limitations of our approach

The comparison of our approach with estimates based on historical distribution ranges showed some diverse results for median and maximum body mass. Median body mass showed no agreement with historical data, whereas maximum body mass showed moderate agreement but also highlighted regional variation. The difference in median body mass can be attributed to the large areas in which median body mass is predicted to have increased by historical data (Fig. S3). This can be caused by the recent loss of small species that is not captured by our model, which is mostly influenced by areas in which large mammals have decreased. Assemblage-level analyses are indeed more influenced by large species as these are more widely distributed than smaller species (Slavenko & Meiri, 2015). Regional differences between the approaches may occur because of limitations in our approach, only based on current data, but also because of limitations in the historical dataset. In fact, although we treated the data derived from the historical dataset as “observed data”, these are necessarily associated to the level of information available, and are a coarse representation of past species distributions. Yet, by using a different approach we reached the same conclusion of Faurby & Araújo (2016) that humans have distorted body mass distributions in mammal assemblages.

One of the limitations in our dataset is that we could not account for the effect of historical over-exploitation, which has likely driven many species to extinction (Faurby & Svenning, 2015; Bartlett et al., 2016). Another potential limitation of our analyses is that we used some environmental variables (e.g., evapotranspiration and primary productivity) that likely reflect human impacts indirectly via habitat modification (fire regimes and agriculture) and climate change. Thus, the minimal impact scenario does not represent pristine conditions, and this makes our estimates of body mass reduction conservative. On the other hand, past extinctions also reflect changes in environmental conditions, not just human impacts, so not all changes in body mass distribution may have been caused by human actions. For example, it is still debated whether early Pleistocene extinctions are to be attributed to climate change, human impact or the combined effect of both (see Koch & Barnosky, 2006; Araujo et al., 2015; Cooper et al., 2015; Bartlett et al., 2016). Similarly, elevation range was used as environmental predictor of mesoscale climatic variation and environmental heterogeneity following previous work (Rodríguez et al., 2006; Rodriguez et al., 2008; Diniz-Filho et al., 2009; Olson et al., 2009). Yet areas with high range of elevation are also likely less accessible to humans, and therefore may also act as a proxy of human impact. Nevertheless, the main scope of our approach is heuristic rather than predictive, and its merit is to illustrate the potential to assess the relative contribution of recent human impact in altering the body mass of mammal species assemblages, and to highlight the need for considering human impact variables to understand macroecological patterns.

4.3. Conclusion

Current body mass distribution is the result of the interaction between natural and anthropogenic factors. Macroecological investigation has traditionally focused on the underlying environmental predictors of natural patterns, but we live in an era of rapid global change. Neglecting the effect of human impact on global macroecological patterns can lead to misleading conclusions on the underlying causes of species distribution (Diniz-Filho et al., 2009; Di Marco & Santini, 2015a; Torres-Romero & Olalla-Tárraga, 2015). Although in many cases macroecological studies are only interested in the underlying environmental predictors of natural patterns, neglecting human impact can lead to misrepresentations and potentially biased estimates of the relative contribution of environmental variables. In fact, human impact and environmental conditions are partly correlated (Table S1), since the former includes processes such as agricultural intensification, urbanisation, and deforestation, which are dependent upon the environmental context. There is a risk that a given environmental variable is found to be a good macroecological predictor, while in fact it is just a distal proxy of suitability for human activities.

Since the ecological determinants of local extinctions may be extremely slow to manifest, being barely noticed in a lifetime, macroecological studies are at risk of incorrectly assuming that the large-scale patterns that we observe today are sufficiently close to pristine natural conditions. In a sense, this may extend the notion of "shifting baseline syndrome" (Papworth et al., 2009) to "shifting macroecological baseline": when the first macroecological investigations started, our understanding of global geographic patterns was based on a situation which was already compromised. Incorporating anthropogenic variables into statistical models of macroecological patterns may permit to account for this issue. However, this is unlikely to completely wipe out the effect of humans from the patterns, due to the inherent difficulty in representing some specific (e.g. hunting) and/or prehistorical human impacts. An informed interpretation that considers possible alterations from the original condition is ultimately necessary.

Acknowledgements

We thank Luigi Maiorano, Francesco Ficetola, Miguel Olalla-Tárraga, Søren Faurby, Jens-Christian Svenning, Yolanda Wiersma and an anonymous reviewer for providing constructive comments that improved the manuscript.

References

Adams D.C. & Church J.O. (2011) The evolution of large-scale body size clines in Plethodon salamanders: evidence of heat-balance or species-specific artifact? *Ecography*, **34**, 1067 1075.

Allendorf F.W. & Hard J.J. (2009) Human-induced evolution caused by unnatural selection through harvest of wild animals. *Proceedings of the National Academy of Sciences of the United States of America*, **106 Suppl**, 9987–9994.

Amante C. & Eakins B.W. (2009) ETOPO1 1 Arc-Minute Global Relief Model:

Procedures, Data Sources and Analysis. *NOAA Technical Memorandum NESDIS NGDC-24. National Geophysical Data Center, NOAA*, .

Araujo B.B.A., Oliveira-Santos L.G.R., Lima-Ribeiro M.S., Diniz-Filho J.A.F., & Fernandez F.A.S. (2015) Bigger kill than chill: The uneven roles of humans and climate on late Quaternary megafaunal extinctions. *Quaternary International*, .

Barnosky A.D. & Lindsey P.A. (2010) Timing of Quaternary megafaunal extinction in South America in relation to human arrival and climate change. *Quaternary International*, **217**, 10–29.

Bartlett L.J., Williams D.R., Prescott G.W., Balmford A., Green R.E., Eriksson A., Valdes P.J., Singarayer J.S., & Manica A. (2016) Robustness despite uncertainty: regional climate data reveal the dominant role of humans in explaining global extinctions of Late Quaternary megafauna. *Ecography*, **39**, 152–161.

Bergmann C. (1847) Über die Verhältnisse der Wärmeökonomie der Thiere zu ihrer Grösse. *Gottinger studien*, **3**, 595–708.

Blackburn T.M., Gaston K.J., & Loder N. (1999) Geographic gradients in body size: a clarification of Bergmann’s rule. *Diversity and Distributions*, **5**, 165–174.

Blackburn T.M. & Hawkins B.A. (2004) Bergmann’s rule and the mammal fauna of northern North America. *Ecography*, **27**, 715–724.

Brown J.H. & Lee A.K. (1969) Bergmann’s rule and climatic adaptation in woodrats (Neotoma). *Evolution*, **23**, 329–338.

Burnham K.P. & Anderson D.R. (2002) *Model Selection and Multimodel Inference: A Practical Information-Theoretic Approach.* Springer, New York.

Calder W.A. (1984) *Size, function and life history.* Harvard University Press, Cambridge, Mass.

Cardillo M., Mace G.M., Jones K.E., Bielby J., Bininda-Emonds O.R.P., Sechrest W., Orme C.D.L., & Purvis A. (2005) Multiple causes of high extinction risk in large mammal species. *Science*, **309**, 1239–1241.

CIESIN & CIAT (2005) Gridded Population of the World, Version 3 (GPWv3): Population Density Grid. NASA Socioeconomic Data and Applications Center (SEDAC), Palisades, NY. .

Cooper A., Turney C., Hughen K.A., Brook B.W., McDonald H.G., & Bradshaw C.J.A. (2015) Abrupt warming events drove Late Pleistocene Holarctic megafaunal turnover. *Science*, **349**, 602–606.

Corlett R. (2007) The impact of hunting on the mammalian fauna of tropical Asian forests. *Biotropica*, **39**, 292–303.

Craigie I.D., Baillie J.E.M., Balmford A., Carbone C., Collen B., Green R.E., & Hutton J.M. (2010) Large mammal population declines in Africa's protected areas. *Biological Conservation*, **143**, 2221–2228.

Damuth J. (1981) Population density and body size in mammals. *Nature*, **290**, 699–700.

Di Marco M., Boitani L., Mallon D., Hoffmann M., Iacucci A., Meijaard E., Visconti P., Schipper J., & Rondinini C. (2014a) A retrospective evaluation of the global decline of carnivores and ungulates. *Conservation Biology*, **28**, 1109–1118.

Di Marco M., Buchanan G.M., Szantoi Z., Holmgren M., Grottolo Marasini G., Gross D., Tranquilli S., Boitani L., & Rondinini C. (2014b) Drivers of extinction risk in African mammals: the interplay of distribution state, human pressure, conservation response and species biology. *Philosophical Transactions of the Royal Society of London B Biological Sciences*, **369**, 20130198.

Di Marco M., Collen B., Rondinini C., & Mace G. (2015) Historical drivers of extinction risk: using past evidence to direct future monitoring. *Proceedings of* *the Royal Society B*, **282**, 20150928.

Di Marco M. & Santini L. (2015a) Human pressures predict species' geographic range size better than biological traits. *Global Change Biology*, **21**, 2169–2178.

Di Marco M. & Santini L. (2015b) Climatic tolerance or geographic breadth: what are we measuring? *Global Change Biology*, **22**, 972–973.

Diniz-Filho J.A.F., Rodrìguez M.A., Bini L.M., Olalla-Tarraga M.A., Cardillo M., Nabout J.C., Hortal J., & Hawkins B.A. (2009) Climate history, human impacts and global body size of Carnivora (Mammalia: Eutheria) at multiple evolutionary scales. *Journal of Biogeography*, **36**, 2222–2236.

Diniz-Filho J.A.F., de Sant'Ana C.E.R., & Bini L.M. (1998) An Eigenvector Method for Estimating Phylogenetic Inertia. *Evolution*, **52**, 1247–1262.

Dirzo R., Young H.S., Galetti M., Ceballos G., Isaac N.J.B., & Collen B. (2014) Defaunation in the Anthropocene. *Science*, **345**, 401–406.

Dunbrack R.L. & Ramsay M.A. (1993) The allometry of mammalian adaptations to seasonal environments: a critique of the fasting endurance hypothesis. *Oikos*, **66**, 336–342.

Ellis E.C., Kaplan J.O., Fuller D.Q., Vavrus S., Goldewijk K.K., & Verburg P.H. (2013) Used planet: A global history. *Proceedings of the National Academy of Sciences*, **110**, 7978–7985.

Faurby S. & Araújo M.B. (2016) Anthropogenic impacts weaken Bergmann's rule. *Ecography*, .

Faurby S. & Svenning J. (2016) Resurrection of the Island Rule: Human-Driven Extinctions Have Obscured a Basic Evolutionary Pattern. *The American Naturalist*, **187**, 812–820.

Faurby S. & Svenning J.C. (2015) Historic and prehistoric human-driven extinctions have reshaped global mammal diversity patterns. *Diversity and Distributions*, **21**, 1155–1166.

Fenchel T. (1974) Intrinsic Rate of Natural Increase: The Relationship with Body Size. *Oecologia*, **14**, 317–326.

Freckleton R.P., Cooper N., & Jetz W. (2011) Comparative Methods as a Statistical Fix: The Dangers of Ignoring an Evolutionary Model. **178**, E10–E17.

Fritz S.A., Bininda-Emonds O.R.P., & Purvis A. (2009) Geographical variation in predictors of mammalian extinction risk: Big is bad, but only in the tropics. *Ecology Letters*, **12**, 538–549.

Goodman S.M., Rasoloarison R.M., & Ganzhorn J.U. (2004) On the specific identification of subfossil Cryptoprocta (Mammalia, Carnivora) from Madagascar. *Zoosystema*, **26**, 129–143.

Hijmans R.J., Cameron S.E., Parra J.L., Jones P.G., & Jarvis A. (2005) Very high resolution interpolated climate surfaces for global land areas. *International Journal of Climatology*, **25**, 1965–1978.

IONIA (2009) Globcover land cover. See http://ionia1.esrin.esa.int . .

IUCN (2015)

James F.C. (1970) Geographic size variation in birds and its relationship to climate. *Ecology*, **51**, 365–390.

Johnson C.N. (2002) Determinants of loss of mammal species during the Late Quaternary “megafauna” extinctions: life history and ecology, but not body size. *Proceedings of the Royal Society B*, **269**, 2221–2227.

Jones K.E., Bielby J., Cardillo M., Fritz S.A., O’Dell J., Orme C.D.L., Safi K., Sechrest W., Boakes E.H., Carbone C., Connolly C., Cutts M.J., Foster J.K., Grenyer R., Habib M., Plaster C.A., Price S.A., Rigby E.A., Rist J., Teacher A., Bininda-Emonds O.R.P., Gittleman J.L., Mace G.M., Purvis A., & Michener W.K. (2009) PanTHERIA: a species-level database of life history, ecology, and geography of extant and recently extinct mammals. *Ecology*, **90**, 2648.

Kissling W.D. & Carl G. (2008) Spatial autocorrelation and the selection of simultaneous autoregressive models. *Global Ecology and Biogeography*, **17**, 59–71.

Koch P.L. & Barnosky A.D. (2006) Late Quaternary Extinctions: State of the Debate. *Annual Review of Ecology and Systematics*, **37**, 215–250.

Legendre P. & Legendre L. (1998) Numerical ecology. *Numerical Ecology Second English Edition*, **20**, 870.

Lewin-Koh N. & Bivand R. (2011) maptools: Tools for reading and handling spatial objects. *R package version …*, 74.

Lindstedt S.L. & Boyce M.S. (1985) Seasonality, fasting endurance, and body size in mammals. *American Naturalist*, **125**, 873–878.

Lister A. & Stuart A.J. (2007) Patterns of Late Quaternary megafaunal extinctions in Europe and northern Asia. *Courier Forschungsinstitut Senckenberg*, **259**, 289–299.

Lyons S.K., Smith F.A., & Brown J.H. (2004) Of mice, mastodons and men: Human-mediated extinctions on four continents. *Evolutionary Ecology Research*, **6**, 339–358.

MacPhee R.D.E. & Grimaldi D.A. (1996) Mammal bones in Dominican amber. *Nature*, **380**, 489–490.

Maurer B. a, Brown J.H., & Rusler R.D. (1992) The Micro and Macro in Body Size Evolution. *Evolution*, **46**, 939–953.

McNab B.K. (2010) Geographic and temporal correlations of mammalian size reconsidered: A resource rule. *Oecologia*, **164**, 13–23.

Meiri S. (2011) Bergmann's Rule – what's in a name? *Global Ecology and Biogeography*, **20**, 203–207.

Meiri S. & Thomas G.H. (2007) The geography of body size – challenges of the interspecific approach. *Global Ecology and Biogeography*, **16**, 689–693.

Milner-Gulland E.J. & Bennet E.L. (2003) Wild meat: the bigger picture. *Trends in Ecology & Evolution*, **18**, 351–357.

Morales-Castilla I., Olalla-Tárraga M.Á., Purvis A., Hawkins B. a., & Rodríguez M.Á. (2012) The Imprint of Cenozoic Migrations and Evolutionary History on the Biogeographic Gradient of Body Size in New World Mammals. *The American Naturalist*, **180**, 246–256.

Morrison J.C., Sechrest W., Dinerstein E., Wilcove D.S., & Lamoreux J.F. (2007) Persistence of large mammal faunas as indicators of global human impacts. *Journal of Mammalogy*, **88**, 1363–1380.

Murray B.R. & Dickman C.R. (2000) Relationships between body size and geographical range size among Australian mammals: has human impact distorted macroecological patterns? *Ecography*, **23**, 92–100.

Nelson A. (2008) Travel Time to Major Cities: A Global Map of Accessibility. *Global Environment Monitoring Unit – Joint Research Centre of the European Commission, Ispra, Italy.*, .

Newbold T., Hudson L.N., Arnell A.P., Contu S., Palma A.D., Ferrier S., Hill S.L.L., Hoskins A.J., Lysenko I., Phillips H.R.P., Burton V.J., Chng C.W.T., Emerson S., Gao D., Pask-Hale G., Hutton J., Jung M., Sanchez-Ortiz, K., Simmons B.I., Whitmee S., & Zhang H. (2016) Has land use pushed terrestrial biodiversity beyond the planetary boundary? A global assessment. *Science*, **353**, 288–291.

Olalla-Tárraga M.A., Torres-Romero E.J., Amado T.F., & Martinez P.A. (2015) Phylogenetic path analysis reveals the importance of niche-related biological traits on geographic range size in mammals. *Global Change Biology*, **21**, 3194–3196.

Olalla- Tárraga M.Á., Bini L.M., Diniz- Filho J.A., & Rodríguez M.Á. (2010) Cross- species and assemblage- based approaches to Bergmann's rule and the biogeography of body size in Plethodon salamanders of eastern North America. *Ecography*, **33**, 362–368.

Olson V.A., Davies R.G., Orme D.L., Thomas G.H., Meiri S., Blackburn T.M., Gaston K.J., Owens I.P.F., & Bennett P.M. (2009) Global biogeography and ecology of body size in birds. *Ecology Letters*, **12**, 249–259.

Pacifici M., Santini L., Di Marco M., Baisero D., Francucci L., Grottolo Marasini G., Visconti P., & Rondinini C. (2013) Generation length for mammals. *Nature Conservation*, **5**, 87–94.

Papworth S.K., Rist J., Coad L., & Milner-Gulland E.J. (2009) Evidence for shifting baseline syndrome in conservation. *Conservation Letters*, **2**, 93–100.

Purvis A., Agapow P.M., Gittleman J.L., & Mace G.M. (2000) Nonrandom Extinction and the Loss of Evolutionary History. *Science*, **288**, 328–330.

R Core Team (2016) R: A language and environment for statistical computing. *R Foundation for Statistical Computing, Vienna, Austria. http://www.R-project.org/*, .

Raffalovich L.E., Deane G.D., Armstrong D., & Tsao H.-S. (2008) Model selection procedures in social research: Monte-Carlo simulation results. *Journal of Applied Statistics*, **35**, 1093–1114.

Ripple W.J., Estes J.A., Beschta R.L., Wilmers C.C., Ritchie E.G., Hebblewhite M., Berger J., Elmhagen B., Letnic M., Nelson M.P., Schmitz O.J., Smith D.W., Wallach A.D., & Wirsing A.J. (2014) Status and Ecological Effects of the World's Largest Carnivores. *Science*, **343**, 1241484.

Ripple W.J., Newsome T.M., Wolf C., Dirzo R., Everatt K.T., Galetti M., Hayward M.W., Kerley G.I.H., Levi T., Lindsey P.A., Macdonald D.W., Malhi Y., Painter L.E., Sandom C.J., Terborgh J., & Van Valkenburgh B. (2015) Collapse of the world's largest herbivores. *Science Advances*, **1**, e1400103.

Ripple W.J. & Van Valkenburgh B. (2010) Linking Top-down Forces to the Pleistocene Megafaunal Extinctions. *BioScience*, **60**, 516–523.

Rodríguez M.A., López-Sañudo I.L., & Hawkins B.A. (2006) The geographic distribution of mammal body size in Europe. *Global Ecology and Biogeography*, **15**, 173–181.

Rodriguez M.A., Olalla-Tárraga M.A., & Hawkins B.A. (2008) Bergmann's rule and the geography of mammal body size in the Western Hemisphere. *Global Ecology and Biogeography*, **17**, 274–283.

Slavenko A. & Meiri S. (2015) Mean body sizes of amphibian species are poorly predicted by climate. *Journal of Biogeography*, 1246–1254.

Smith F.A., Lyons K., Morgan Ernest S.K., Jones K.E., Kaufman D.M., Dayan T., Marquet P.A., Brown J.H., & Haskell J.P. (2003) Body mass of late quaternary mammals. *Ecology*, **84**, 3403–3403.

Smith F.A. & Lyons S.K. (2011) How big should a mammal be? A macroecological look at mammalian body size over space and time. *Philosophical Transactions of the Royal Society of London B Biological Sciences*, **366**, 2364–2378.

Sodhi N.S., Koh L.P., Brook B.W., & Ng P.K.L. (2004) Southeast Asian biodiversity: An impending disaster. *Trends in Ecology and Evolution*, **19**, 654–660.

Speakman J.R. & Król E. (2010) Maximal heat dissipation capacity and hyperthermia risk: neglected key factors in the ecology of endotherms. *Journal of Animal Ecology*, **79**, 726–746.

Torres-Romero E.J. & Olalla-Tárraga M.A. (2015) Untangling human and environmental effects on geographical gradients of mammal species richness: a global and regional evaluation. *Journal of Animal Ecology*, **84**, 851–860.

Villalobos F., Olalla-Tárraga M.Á., Cianciaruso M. V., Rangel T.F., & Diniz-Filho J.A.F. (2016) Global patterns of mammalian co-occurrence: phylogenetic and body size structure within species ranges. *Journal of Biogeography*, 1–11.

van Vuure C. (2005) *Retracing the aurochs: history, morphology and ecology of an extinct wild ox.* Pensoft, Sofia-Moscow.

Woinarski J.C., Burbidge A.A., & Harrison P.L. (2015) Ongoing unraveling of a continental fauna: Decline and extinction of Australian mammals since European settlement. *Proceedings of the National Academy of Sciences*, **112**, 4531–4540.

Woodroffe R. (2000) Predators and people: using human densities to interpret declines of large carnivores. *Animal Conservation*, **3**, 165–173.

Table 1. Comparison of SAR models explaining the observed distribution of median (Med), maximum body mass represented as the 90th percentile (Max) and body mass skewness (Skew). Only the most supported models are shown here ($\omega \geq 0.1$; see Table S5 for all models). df = degree of freedom; BIC = Bayesian Information Criterion; ΔBIC = difference in BIC with the best model; ω = BIC weight; R^2_{sp}= variance explained by the fixed factor and the spatial autocorrelation combined; R^2_{nsp}= variance explained by the fixed factors only. C1-2 = First two principal components explaining ~ 65% of the variance of environmental variables and order richness; Acc = Accessibility; pAg = Percentage of agricultural areas; PD = Population density; YFU = Year from first land use; ISL = factor to classify cells as islands (ISL1 = <25,000 km^2; ISL2= <100,000 km^2; ISL3 = <500,000 km^2; ISL4 = <750,000,000 km^2).

Formula	**df**	**BIC**	**ΔBIC**	**ω**	**R^2_{sp}**	**R^2_{nsp}**	**Int**	**C1**	**C2**	**Acc**	**YFU**	**pAg**	**ISL4**
Med ~ C1 + C2 + YFU + Acc	7	-8564.03	0	0.95	0.94	0.08	-0.354 (0.019) *	0.011 (0.007)	-0.071 (0.011) *	0.032 (0.005) *	-0.017 (0.004) *	-	-
Max ~ ISL4 + C1 + C2 + Acc	7	-17291.36	0	0.94	0.92	0.17	1.466 (0.014) *	0.000 (0.005)	0.035 (0.009) *	0.037 (0.004) *	-	-	-0.183 (0.017) *
Skew ~ ISL4 + C1 + C2 + YFU + Acc	8	-39027.21	0	0.43	0.91	0.30	0.561 (0.005) *	-0.042 (0.002)*	-0.013 (0.004) *	-0.004 (0.002) *	0.003 (0.001)	-	-0.091 (0.007) *
Skew ~ ISL4 + C1 + C2 + Acc + pAg	8	-39026.66	0.54	0.33	0.91	0.30	0.561 (0.005) *	-0.042 (0.002) *	-0.012 (0.004) *	-0.004 (0.002) *	-	0.003 (0.002)	-0.091 (0.007) *
Skew ~ ISL4 + C1 + C2 + Acc	7	-39025.27	1.94	0.16	0.91	0.30	0.561 (0.005) *	-0.043 (0.002) *	-0.013 (0.004) *	-0.005 (0.002) *	-	-	-0.090 (0.007) *

Table 2. Difference (Δ) of the estimated coefficients and standard errors (in brackets) of intercepts and slopes describing the relationship between latitude and predicted body mass according to the two scenarios of human impact (*Body mass ~ Human_Impact + Latitude:Human_Impact*). Δ = Coefficient for the minimal impact scenario - Coefficient for the observed impact scenario; N = Northern hemisphere; S = Southern hemisphere; * = P-value <0.05; df = degree of freedom. Significance indicates a significant alteration of the relationship between latitude and body mass. Standard errors equal to zero are due to the rounding of the fourth decimal value.

Model	**Δ Intercept**	**Δ Slope latitude**
Med (Northern hemisphere)	0.214(0.003)*	-0.002(1x10^{-4})*
Med (0° - 20°)	0.123(0.004)*	0.002(3x10^{-4})*
Med (Southern hemisphere)	0.128(0.002)*	-4x10^{-4}(1x10^{-4})*
Max (Northern hemisphere)	12.670(0.121)*	-0.051(0.002)*
Max (0°- 20°)	8.752(0.127)*	0.049(0.011)*
Max (Southern hemisphere)	8.182(0.105)*	-0.070(0.005)*

Figures

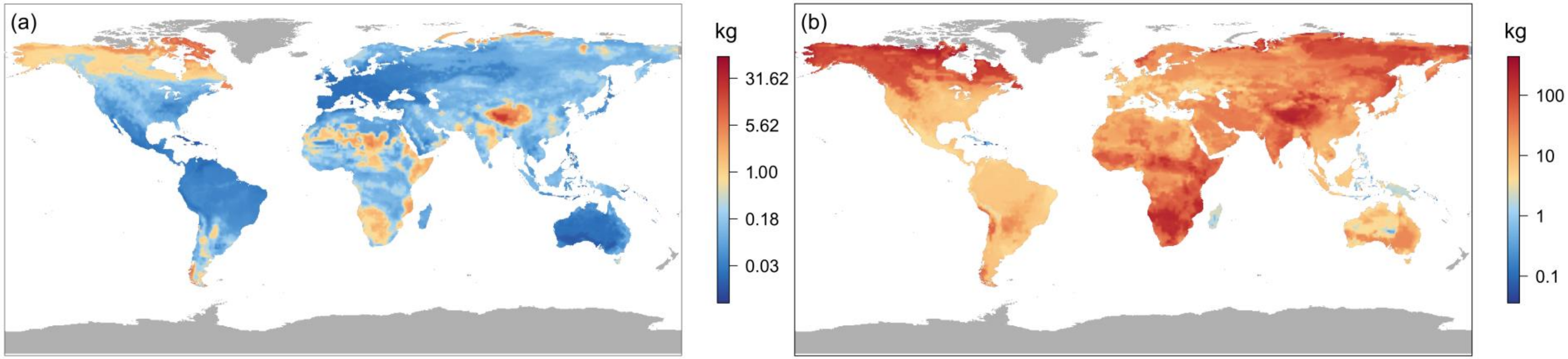

Fig. 1. Median (a) and maximum (b) values of body mass in terrestrial mammals (values on a log-10 scale aggregated into grids of 1 degree). Cells with ≤5 species are represented in grey (and were not considered in the analyses). The maximum is reported as the 90% percentile of the body mass distribution (only for cells with >10 species).

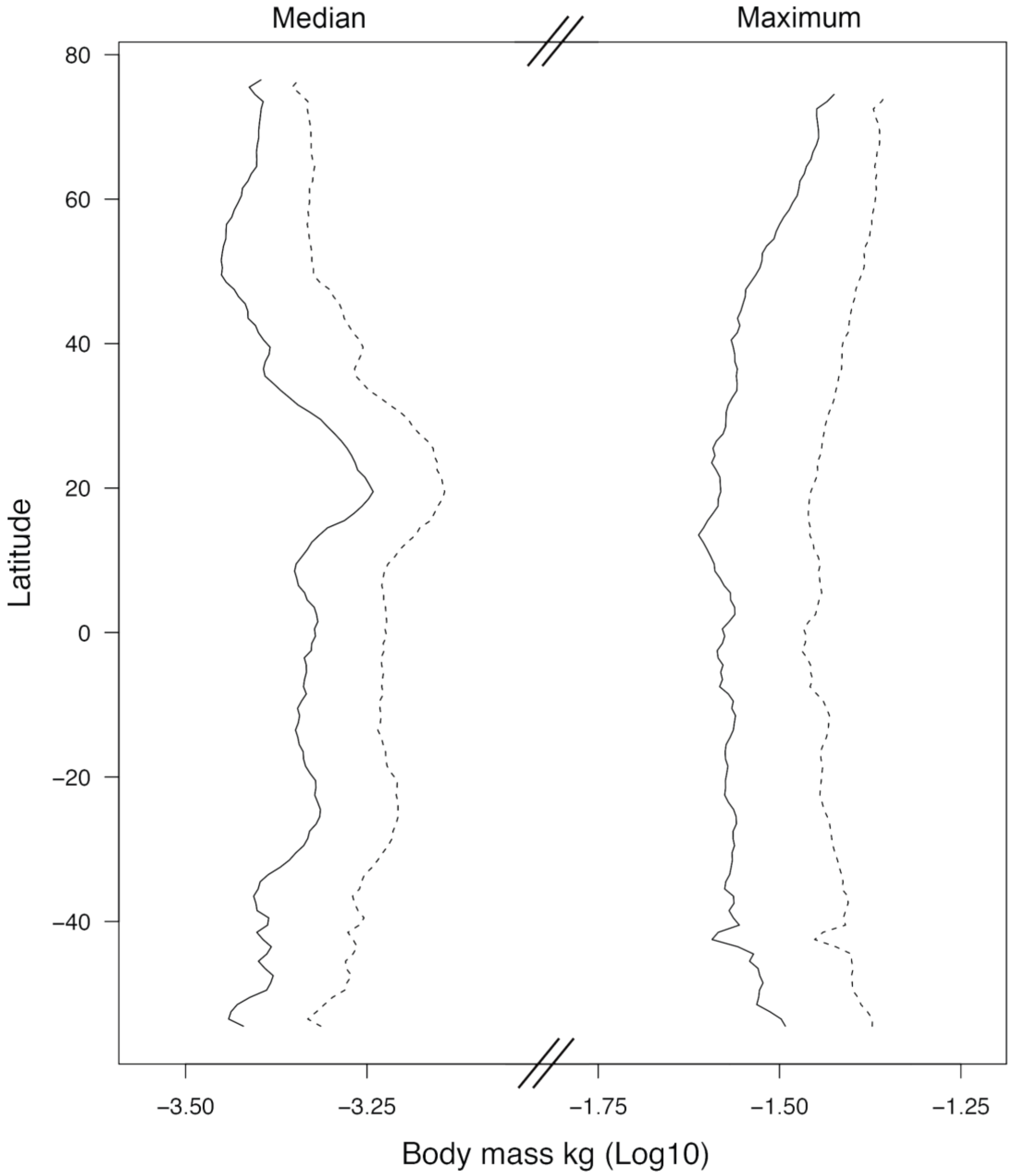

Fig. 2. Relationship between latitude and median and maximum body mass. Continuous lines represent the predictions with human impact, whereas dashed lines the predictions without human impact.

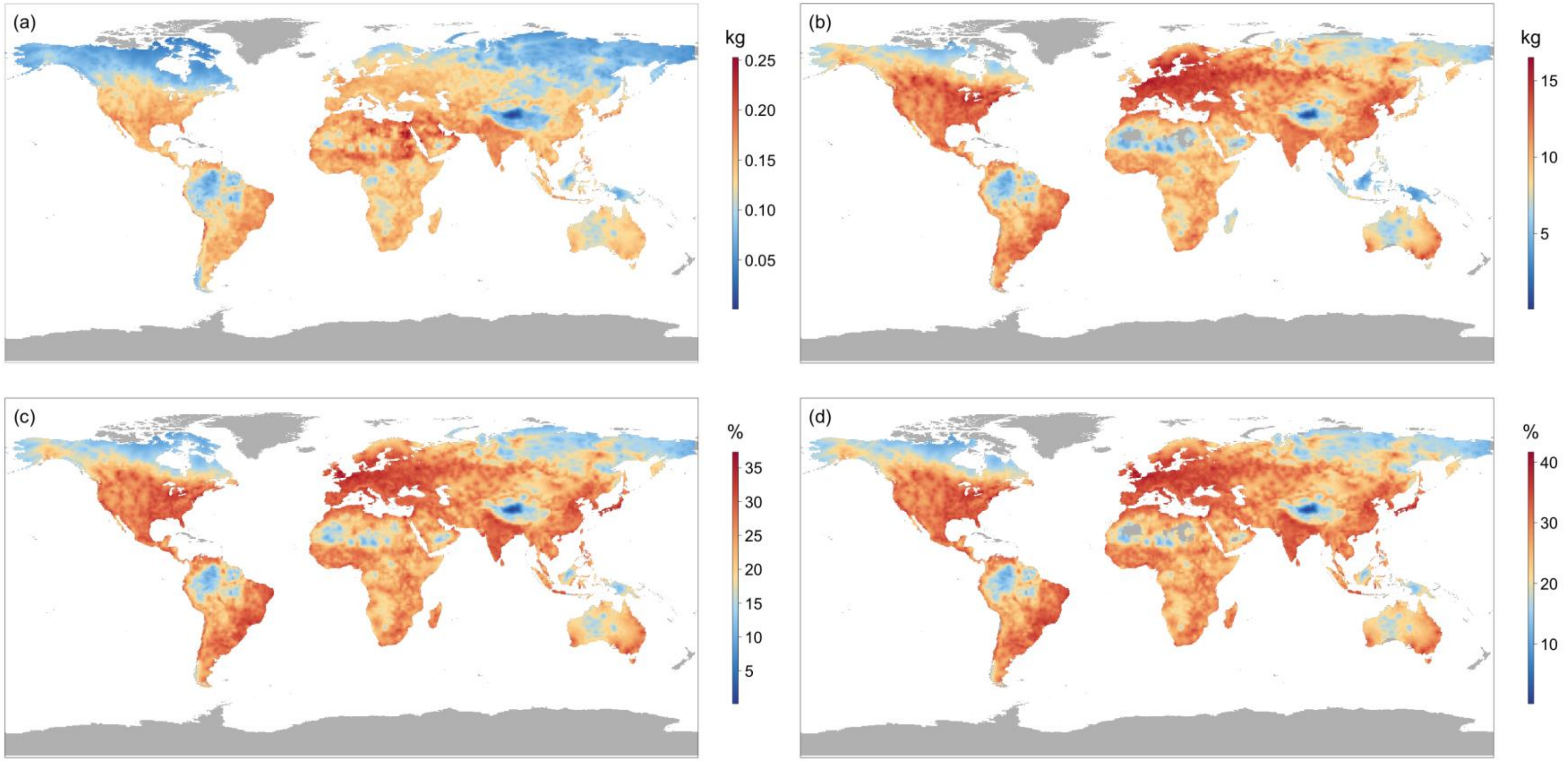

Fig. 3. Difference in predicted body mass between the observed and minimal impact scenarios. The plots report the absolute difference in median (a) and maximum (b) body mass values, and the relative (%) difference in median (c) and maximum (d) body mass values. Cells with ≤5 and ≤10 species are represented in grey for median and maximum respectively (and were not considered in the analyses).

SUPPORTING INFORMATION

Additional Supporting Information may be found in the online version of this article:

Table S1. Correlation matrix of all variables used in the study.

Table S2. Importance values and broken-stick distribution of the principal components.

Table S3. Loadings of variables on the principal components.

Table S4. Moran Index test results for OLS model's residuals.

Table S5. Comparison of models explaining the observed distribution of median, maximum body mass and body mass skewness based on BIC.

Table S6. Coefficient estimates for all models tested.

Table S7. Comparison of models explaining the observed distribution of median, maximum body mass and body mass skewness based on AIC.

Fig. S1. Correlograms for the null models of median and maximum body mass, and skewness in body mass distribution.

Fig. S2. Median (a) and maximum (b) values of body mass in terrestrial mammals estimated considering the historical geographic ranges from Faurby & Svenning (2015; values aggregated into grids of 1 degree, and log10-transformed). The maximum is reported as the 97.5% percentile of the body mass distribution.

Fig. S3. Difference in median (a) and maximum (b) body mass between current and historical body mass distributions, estimated considering the historical geographic ranges from Faurby & Svenning (2015; values aggregated into grids of 1 degree, and log10-transformed). Black areas are estimated to have increased mean and maximum body mass.

Biosketch

Luca Santini is a postdoctoral research fellow and his research primarily focuses on the link between macroecology and conservation biogeography, with main interests in species biological traits and their natural covariation, species distribution, patterns of spatial ecology, and the effect of anthropogenic impact in natural patterns.

Supplementary Materials

Shifting baseline in macroecology? Unraveling the influence of human impact on mammalian body mass

Luca Santini[1,2*], Manuela González-Suárez[3,4], Carlo Rondinini[2], Moreno Di Marco[5,6]

[1] Department of Environmental Science, Radboud University, P.O. Box 9010, NL-6500 GL, Nijmegen, The Netherlands

[2] Global Mammal Assessment program, Department of Biology and Biotechnologies, Sapienza Università di Roma, Viale dell'Università 32, 00185 Rome, Italy

[3] Department of Conservation Biology, Estación Biológica de Doñana - CSIC, 41092 Seville, Spain.

[4] Ecology and Evolutionary Biology, School of Biological Sciences, University of Reading, Whiteknights, Reading, Berkshire, RG6 6AS, UK

[5] ARC Centre of Excellence for Environmental Decision, Centre for Biodiversity and Conservation Science, The University of Queensland, St Lucia, QLD 4072 (Brisbane, Australia).

[6] School of Earth and Environmental Sciences, The University of Queensland, St Lucia, QLD 4072 (Brisbane, Australia).

Fig. S1. Correlograms for the null models of (a) median and (b) maximum body mass, and (c) skewness in body mass distribution.

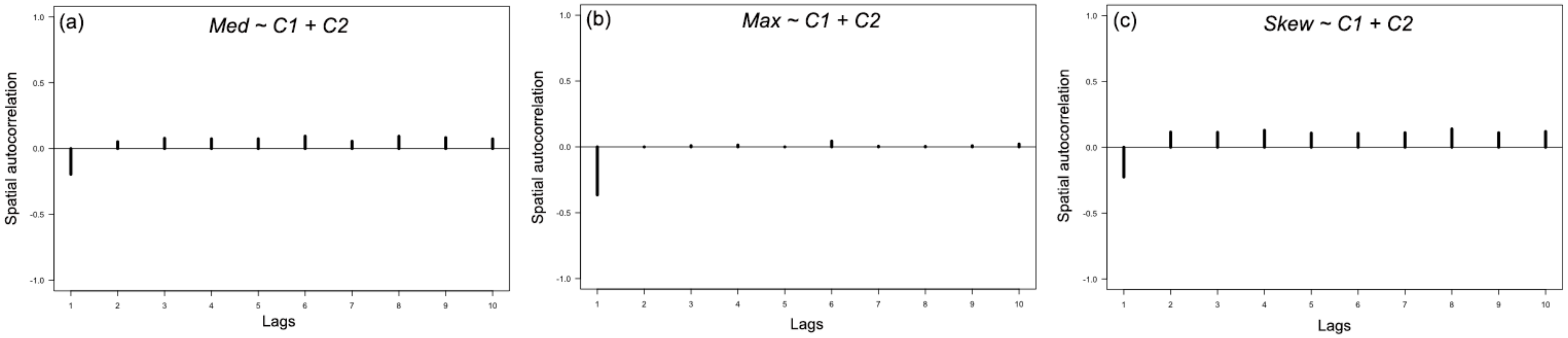

Fig. S2. Median (a) and maximum (b) values of body mass in terrestrial mammals estimated considering the historical geographic ranges from Faurby & Svenning (2015; values aggregated into grids of 1 degree, and log10-transformed). The maximum is reported as the 97.5% percentile of the body mass distribution.

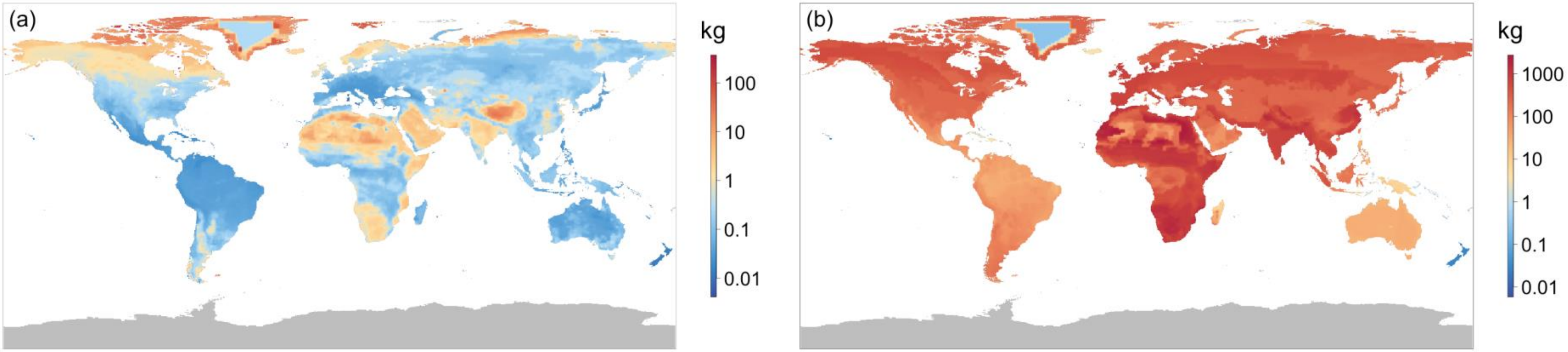

Fig. S3. Difference in median (a) and maximum (b) body mass between current and historical body mass distributions, estimated considering the historical geographic ranges from Faurby & Svenning (2015; values aggregated into grids of 1 degree, and log10- transformed). Black areas are estimated to have increased mean and maximum body mass.

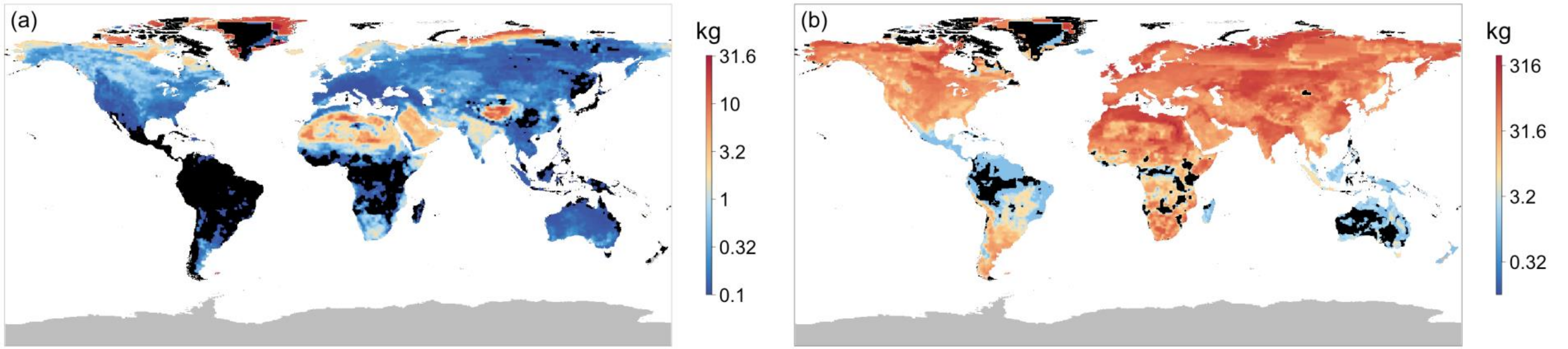

Table S1. Correlation matrix of all variables used in the study. pAg = Proportion of agricultural areas; PD = Population density; Acc = Accessibility; YFU = Year from first land use; Rich_O = Order richness; T = Mean annual temperature; Tcq = Mean temperature of the coldest quarter; Twq = Mean temperature of the warmest quarter; P = Mean annual precipitations; Pwq = Precipitations of the warmest quarter; Pdq = Precipitations of the driest quarter; TGR = Time since last glacial retreat; ER = Elevation range; NDVI = Normalized Difference of Vegetation Index; NDVI_cv = Within year coefficient of variation of the Normalized Difference of Vegetation Index; AET = Actual evapotraspiration; PET = Potential evapotraspiration. Correlation coefficients higher than 0.6 (or lower than -0.6) are highlighted in bold.

	pAg	**PD**	**Acc**	**YFU**	**Rich_O**	**T**	**Tcq**	**Twq**	**P**	**Pwq**	**Pdq**	**TGR**	**ER**	**NDVI**	**NDVI_cv**
PD	**0.71**														
Acc	**-0.68**	**-0.74**													
YFU	**0.73**	**0.66**	**-0.70**												
Rich_O	0.49	0.48	-0.31	0.44											
T	0.48	0.59	-0.41	0.42	0.59										
Tcq	0.49	0.58	-0.39	0.42	**0.62**	**0.98**									
Twq	0.38	0.55	-0.41	0.37	0.46	**0.93**	**0.85**								
P	0.4	0.25	-0.24	0.34	0.45	0.09	0.16	-0.07							
Pwq	0.42	0.29	-0.22	0.36	0.50	0.15	0.22	-0.01	**0.98**						
Pdq	0.15	-0.04	-0.09	0.1	0.03	-0.3	-0.24	-0.4	**0.64**	0.53					
TGR	0.39	0.56	-0.28	0.3	0.32	0.47	0.42	0.52	-0.02	0.03	-0.18				
ER	0.16	0.17	-0.04	0.12	0.05	-0.06	-0	-0.18	0.11	0.13	0.13	0.08			
NDVI	0.22	0.14	-0.17	0.19	0.26	-0.14	-0.1	-0.23	**0.68**	**0.65**	0.56	-0.07	-0.02		
NDVI_cv	0.39	0.24	-0.39	0.41	0.25	-0.06	-0.03	-0.15	0.58	0.56	0.45	-0.12	0.05	**0.65**	
AET	0.26	0.23	-0.17	0.24	0.38	0.16	0.16	0.13	0.39	0.41	0.18	0.15	-0.03	0.32	0.23

Table S2. Importance values and broken-stick distribution of the principal components. PCA components with larger percentages of accumulated variance than the broken-stick variances are significant (Legendre and Legendre, 1998).

	Comp.1	**Comp.2**	**Comp.3**	**Comp.4**	**Comp.5**	**Comp.6**	**Comp.7**	**Comp.8**	**Comp.9**	**Comp.10**	**Comp.11**	**Comp.12**
Eigenvalue	3.99	3.72	1.07	0.83	0.66	0.57	0.42	0.34	0.28	0.10	0.01	0.00
Standard deviation	2.00	1.93	1.04	0.91	0.81	0.75	0.65	0.58	0.53	0.31	0.11	0.03
% of Variance	33.26	31.03	8.96	6.88	5.51	4.75	3.53	2.84	2.35	0.79	0.10	0.01
Cumulative %	33.26	64.29	73.25	80.13	85.64	90.38	93.92	96.75	99.10	99.90	99.99	100.00
Broken-stick %	25.86	17.53	13.36	10.58	8.50	6.83	5.44	4.25	3.210	2.29	1.45	0.69
Broken-stick cumulative %	25.86	43.39	56.75	67.33	75.83	82.66	88.10	92.36	95.57	97.85	99.31	100.00

Table S3. Loadings of variables on the principal components (C).

	C1	**C2**	**C3**	**C4**	**C5**	**C6**	**C7**	**C8**	**C9**	**C10**	**C11**	**C12**	**C13**
Taxonomic Order richness	-0.35	-0.22	0.03	0.00	-0.20	-0.16	0.60	0.60	-0.16	0.11	-0.02	-0.00	-0.35
Mean annual temperature	-0.19	-0.46	-0.02	-0.2	-0.05	0.04	-0.22	-0.00	0.11	-0.14	0.05	0.79	-0.19
Mean temperature of the coldest quarter	-0.22	-0.43	0.03	-0.24	-0.11	0.07	-0.19	0.02	0.14	-0.57	0.02	-0.55	-0.22
Mean temperature of the warmest quarter	-0.11	-0.47	-0.12	-0.08	0.08	0.02	-0.27	-0.07	0.06	0.77	-0.05	-0.26	-0.11
Mean annual precipitations	-0.45	0.15	0.03	-0.10	-0.05	0.29	0.12	-0.33	-0.11	0.01	-0.74	0.03	-0.45
Precipitations of the wettest quarter	-0.45	0.11	0.05	-0.08	-0.08	0.21	0.23	-0.45	-0.14	0.09	0.66	-0.03	-0.45
Precipitations of the driest quarter	-0.25	0.32	0.08	-0.05	0.16	0.52	-0.43	0.56	-0.12	0.05	0.12	-0.00	-0.25
Time since last glacial retreat	-0.10	-0.3	0.26	0.46	0.75	0.05	0.13	-0.06	-0.16	-0.14	-0.01	0.00	-0.10
Elevation range	-0.05	0.06	0.92	-0.02	-0.20	-0.21	-0.14	-0.02	0.17	0.13	-0.02	-0.00	-0.05
Primary productivity	-0.35	0.24	-0.16	0.01	0.28	-0.21	0.09	0.06	0.81	0.03	0.02	0.00	-0.35
Primary productivity seasonality	-0.32	0.20	-0.11	-0.23	0.21	-0.69	-0.31	-0.01	-0.42	-0.05	-0.00	-0.01	-0.32
Actual evapotranspiration	-0.27	-0.02	-0.15	0.79	-0.43	-0.11	-0.30	-0.03	0.00	-0.05	-0.00	-0.00	-0.27

Table S4. Moran Index test results for OLS model's residuals. The Moran Index test the null hypothesis of no spatial autocorrelation. C1-2 = First two principal components explaining ~ 65% of the variance of environmental variables and order richness; Acc = Accessibility; pAg = Percentage of agricultural areas; PD = Population density; YFU = Year from first land use; ISL = factor to classify cells as islands (ISL1 = <25,000 km^2; ISL2= <100,000 km^2; ISL3 = <500,000 km^2; ISL4 = <750,000,000 km^2).

Model	**Observed**	**Expectation**	**Variance**	**p-value**
Med ~ C1+C2	0.9241	-0.0002	3.7465×10^{-5}	$< 2.2\times10^{-16}$
Med ~ C1+C2+Acc	0.9031	-0.0003	3.7461×10^{-5}	$< 2.2\times10^{-16}$
Med ~ C1+C2+pAg	0.9179	-0.0003	3.7462×10^{-5}	$< 2.2\times10^{-16}$
Med ~ C1+C2+PD	0.9068	-0.0003	3.7461×10^{-5}	$< 2.2\times10^{-16}$
Med ~ C1+C2+Acc+pAg	0.9026	-0.0003	3.7458×10^{-5}	$< 2.2\times10^{-16}$
Med ~ C1+C2+YFU	0.9162	-0.0003	3.7461×10^{-5}	$< 2.2\times10^{-16}$
Med ~ C1+C2+YFU+PD	0.908	-0.0003	3.7457×10^{-5}	$< 2.2\times10^{-16}$
Med ~ C1+C2+YFU+Acc	0.9014	-0.0003	3.7458×10^{-5}	$< 2.2\times10^{-16}$
Med ~ ISL1+C1+C2	0.9241	-0.0002	3.7463×10^{-5}	$< 2.2\times10^{-16}$
Med ~ ISL1+C1+C2+Acc	0.9031	-0.0003	3.7459×10^{-5}	$< 2.2\times10^{-16}$
Med ~ ISL1+C1+C2+pAg	0.918	-0.0003	3.7459×10^{-5}	$< 2.2\times10^{-16}$
Med ~ ISL1+C1+C2+PD	0.9068	-0.0003	3.7459×10^{-5}	$< 2.2\times10^{-16}$
Med ~ ISL1+C1+C2+Acc+pAg	0.9025	-0.0003	3.7455×10^{-5}	$< 2.2\times10^{-16}$
Med ~ ISL1+C1+C2+YFU	0.9162	-0.0003	3.7459×10^{-5}	$< 2.2\times10^{-16}$
Med ~ ISL1+C1+C2+YFU+PD	0.9081	-0.0003	3.7455×10^{-5}	$< 2.2\times10^{-16}$
Med ~ ISL1+C1+C2+YFU+Acc	0.9014	-0.0003	3.7455×10^{-5}	$< 2.2\times10^{-16}$
Med ~ ISL2+C1+C2	0.9241	-0.0002	3.7461×10^{-5}	$< 2.2\times10^{-16}$
Med ~ ISL2+C1+C2+Acc	0.903	-0.0003	3.7457×10^{-5}	$< 2.2\times10^{-16}$
Med ~ ISL2+C1+C2+pAg	0.9178	-0.0003	3.7457×10^{-5}	$< 2.2\times10^{-16}$
Med ~ ISL2+C1+C2+PD	0.9066	-0.0003	3.7456×10^{-5}	$< 2.2\times10^{-16}$
Med ~ ISL2+C1+C2+Acc+pAg	0.9025	-0.0004	3.7453×10^{-5}	$< 2.2\times10^{-16}$

Model	Observed	Expectation	Variance	p-value
Med ~ ISL2+C1+C2+YFU	0.916	-0.0003	3.7457×10^{-5}	$< 2.2\times10^{-16}$
Med ~ ISL2+C1+C2+YFU+PD	0.9079	-0.0004	3.7453×10^{-5}	$< 2.2\times10^{-16}$
Med ~ ISL2+C1+C2+YFU+Acc	0.9014	-0.0004	3.7453×10^{-5}	$< 2.2\times10^{-16}$
Med ~ ISL3+C1+C2	0.9241	-0.0003	3.7460×10^{-5}	$< 2.2\times10^{-16}$
Med ~ ISL3+C1+C2+Acc	0.9031	-0.0003	3.7456×10^{-5}	$< 2.2\times10^{-16}$
Med ~ ISL3+C1+C2+pAg	0.918	-0.0003	3.7457×10^{-5}	$< 2.2\times10^{-16}$
Med ~ ISL3+C1+C2+PD	0.9067	-0.0003	3.7456×10^{-5}	$< 2.2\times10^{-16}$
Med ~ ISL3+C1+C2+Acc+pAg	0.9025	-0.0004	3.7453×10^{-5}	$< 2.2\times10^{-16}$
Med ~ ISL3+C1+C2+YFU	0.9162	-0.0003	3.7456×10^{-5}	$< 2.2\times10^{-16}$
Med ~ ISL3+C1+C2+YFU+PD	0.908	-0.0004	3.7452×10^{-5}	$< 2.2\times10^{-16}$
Med ~ ISL3+C1+C2+YFU+Acc	0.9014	-0.0004	3.7453×10^{-5}	$< 2.2\times10^{-16}$
Med ~ ISL4+C1+C2	0.9214	-0.0003	3.7461×10^{-5}	$< 2.2\times10^{-16}$
Med ~ ISL4+C1+C2+Acc	0.9012	-0.0003	3.7457×10^{-5}	$< 2.2\times10^{-16}$
Med ~ ISL4+C1+C2+pAg	0.9135	-0.0003	3.7457×10^{-5}	$< 2.2\times10^{-16}$
Med ~ ISL4+C1+C2+PD	0.9033	-0.0003	3.7456×10^{-5}	$< 2.2\times10^{-16}$
Med ~ ISL4+C1+C2+Acc+pAg	0.9013	-0.0004	3.7453×10^{-5}	$< 2.2\times10^{-16}$
Med ~ ISL4+C1+C2+YFU	0.9127	-0.0003	3.7457×10^{-5}	$< 2.2\times10^{-16}$
Med ~ ISL4+C1+C2+YFU+PD	0.9046	-0.0004	3.7453×10^{-5}	$< 2.2\times10^{-16}$
Med ~ ISL4+C1+C2+YFU+Acc	0.9002	-0.0004	3.7453×10^{-5}	$< 2.2\times10^{-16}$
Max ~ C1+C2	0.8983	-0.0002	3.8086×10^{-5}	$< 2.2\times10^{-16}$
Max ~ C1+C2+Acc	0.8789	-0.0003	3.8082×10^{-5}	$< 2.2\times10^{-16}$
Max ~ C1+C2+pAg	0.8818	-0.0003	3.8082×10^{-5}	$< 2.2\times10^{-16}$
Max ~ C1+C2+PD	0.8855	-0.0003	3.8082×10^{-5}	$< 2.2\times10^{-16}$
Max ~ C1+C2+Acc+pAg	0.8779	-0.0003	3.8078×10^{-5}	$< 2.2\times10^{-16}$
Max ~ C1+C2+YFU	0.89	-0.0003	3.8082×10^{-5}	$< 2.2\times10^{-16}$
Max ~ C1+C2+YFU+PD	0.8862	-0.0003	3.8078×10^{-5}	$< 2.2\times10^{-16}$

Model	**Observed**	**Expectation**	**Variance**	**p-value**
Max ~ C1+C2+YFU+Acc	0.8782	-0.0003	3.8078×10^{-5}	$< 2.2\times10^{-16}$
Max ~ ISL1+C1+C2	0.8987	-0.0002	3.8083×10^{-5}	$< 2.2\times10^{-16}$
Max ~ ISL1+C1+C2+Acc	0.8791	-0.0003	3.8079×10^{-5}	$< 2.2\times10^{-16}$
Max ~ ISL1+C1+C2+pAg	0.8825	-0.0003	3.8079×10^{-5}	$< 2.2\times10^{-16}$
Max ~ ISL1+C1+C2+PD	0.8861	-0.0003	3.8079×10^{-5}	$< 2.2\times10^{-16}$
Max ~ ISL1+C1+C2+Acc+pAg	0.8783	-0.0004	3.8075×10^{-5}	$< 2.2\times10^{-16}$
Max ~ ISL1+C1+C2+YFU	0.8907	-0.0003	3.8079×10^{-5}	$< 2.2\times10^{-16}$
Max ~ ISL1+C1+C2+YFU+PD	0.8868	-0.0003	3.8075×10^{-5}	$< 2.2\times10^{-16}$
Max ~ ISL1+C1+C2+YFU+Acc	0.8781	-0.0003	3.8075×10^{-5}	$< 2.2\times10^{-16}$
Max ~ ISL2+C1+C2	0.8987	-0.0003	3.8081×10^{-5}	$< 2.2\times10^{-16}$
Max ~ ISL2+C1+C2+Acc	0.8799	-0.0003	3.8077×10^{-5}	$< 2.2\times10^{-16}$
Max ~ ISL2+C1+C2+pAg	0.8826	-0.0003	3.8077×10^{-5}	$< 2.2\times10^{-16}$
Max ~ ISL2+C1+C2+PD	0.8865	-0.0003	3.8077×10^{-5}	$< 2.2\times10^{-16}$
Max ~ ISL2+C1+C2+Acc+pAg	0.8788	-0.0004	3.8073×10^{-5}	$< 2.2\times10^{-16}$
Max ~ ISL2+C1+C2+YFU	0.891	-0.0003	3.8077×10^{-5}	$< 2.2\times10^{-16}$
Max ~ ISL2+C1+C2+YFU+PD	0.8872	-0.0004	3.8073×10^{-5}	$< 2.2\times10^{-16}$
Max ~ ISL2+C1+C2+YFU+Acc	0.8788	-0.0004	3.8073×10^{-5}	$< 2.2\times10^{-16}$
Max ~ ISL3+C1+C2	0.8993	-0.0003	3.8081×10^{-5}	$< 2.2\times10^{-16}$
Max ~ ISL3+C1+C2+Acc	0.881	-0.0003	3.8077×10^{-5}	$< 2.2\times10^{-16}$
Max ~ ISL3+C1+C2+pAg	0.8834	-0.0003	3.8077×10^{-5}	$< 2.2\times10^{-16}$
Max ~ ISL3+C1+C2+PD	0.8875	-0.0003	3.8077×10^{-5}	$< 2.2\times10^{-16}$
Max ~ ISL3+C1+C2+Acc+pAg	0.8797	-0.0004	3.8073×10^{-5}	$< 2.2\times10^{-16}$
Max ~ ISL3+C1+C2+YFU	0.8917	-0.0003	3.8077×10^{-5}	$< 2.2\times10^{-16}$
Max ~ ISL3+C1+C2+YFU+PD	0.8881	-0.0004	3.8073×10^{-5}	$< 2.2\times10^{-16}$
Max ~ ISL3+C1+C2+YFU+Acc	0.88	-0.0004	3.8073×10^{-5}	$< 2.2\times10^{-16}$
Max ~ ISL4+C1+C2	0.8967	-0.0003	3.8081×10^{-5}	$< 2.2\times10^{-16}$
Max ~ ISL4+C1+C2+Acc	0.8759	-0.0003	3.8077×10^{-5}	$< 2.2\times10^{-16}$

Model	**Observed**	**Expectation**	**Variance**	**p-value**
Max ~ ISL4+C1+C2+pAg	0.8816	-0.0003	3.8077×10^{-5}	$< 2.2\times10^{-16}$
Max ~ ISL4+C1+C2+PD	0.8849	-0.0003	3.8077×10^{-5}	$< 2.2\times10^{-16}$
Max ~ ISL4+C1+C2+Acc+pAg	0.8757	-0.0004	3.8073×10^{-5}	$< 2.2\times10^{-16}$
Max ~ ISL4+C1+C2+YFU	0.8887	-0.0003	3.8077×10^{-5}	$< 2.2\times10^{-16}$
Max ~ ISL4+C1+C2+YFU+PD	0.8854	-0.0004	3.8073×10^{-5}	$< 2.2\times10^{-16}$
Max ~ ISL4+C1+C2+YFU+Acc	0.8742	-0.0004	3.8073×10^{-5}	$< 2.2\times10^{-16}$
Skew ~ C1+C2	0.81	-0.0002	3.7465×10^{-5}	$< 2.2\times10^{-16}$
Skew ~ C1+C2+Acc	0.7862	-0.0003	3.7461×10^{-5}	$< 2.2\times10^{-16}$
Skew ~ C1+C2+pAg	0.7988	-0.0003	3.7462×10^{-5}	$< 2.2\times10^{-16}$
Skew ~ C1+C2+PD	0.7881	-0.0003	3.7461×10^{-5}	$< 2.2\times10^{-16}$
Skew ~ C1+C2+Acc+pAg	0.7875	-0.0003	3.7458×10^{-5}	$< 2.2\times10^{-16}$
Skew ~ C1+C2+YFU	0.7916	-0.0003	3.7461×10^{-5}	$< 2.2\times10^{-16}$
Skew ~ C1+C2+YFU+PD	0.7867	-0.0003	3.7457×10^{-5}	$< 2.2\times10^{-16}$
Skew ~ C1+C2+YFU+Acc	0.7865	-0.0003	3.7458×10^{-5}	$< 2.2\times10^{-16}$
Skew ~ ISL1+C1+C2	0.8086	-0.0002	3.7463×10^{-5}	$< 2.2\times10^{-16}$
Skew ~ ISL1+C1+C2+Acc	0.7842	-0.0003	3.7459×10^{-5}	$< 2.2\times10^{-16}$
Skew ~ ISL1+C1+C2+pAg	0.7979	-0.0003	3.7459×10^{-5}	$< 2.2\times10^{-16}$
Skew ~ ISL1+C1+C2+PD	0.7866	-0.0003	3.7459×10^{-5}	$< 2.2\times10^{-16}$
Skew ~ ISL1+C1+C2+Acc+pAg	0.7858	-0.0003	3.7455×10^{-5}	$< 2.2\times10^{-16}$
Skew ~ ISL1+C1+C2+YFU	0.7905	-0.0003	3.7459×10^{-5}	$< 2.2\times10^{-16}$
Skew ~ ISL1+C1+C2+YFU+PD	0.7854	-0.0003	3.7455×10^{-5}	$< 2.2\times10^{-16}$
Skew ~ ISL1+C1+C2+YFU+Acc	0.7849	-0.0003	3.7455×10^{-5}	$< 2.2\times10^{-16}$
Skew ~ ISL2+C1+C2	0.8098	-0.0002	3.7461×10^{-5}	$< 2.2\times10^{-16}$
Skew ~ ISL2+C1+C2+Acc	0.7861	-0.0003	3.7457×10^{-5}	$< 2.2\times10^{-16}$
Skew ~ ISL2+C1+C2+pAg	0.7987	-0.0003	3.7457×10^{-5}	$< 2.2\times10^{-16}$
Skew ~ ISL2+C1+C2+PD	0.788	-0.0003	3.7456×10^{-5}	$< 2.2\times10^{-16}$

Model	Observed	Expectation	Variance	p-value
Skew ~ ISL2+C1+C2+Acc+pAg	0.7874	-0.0004	3.7453×10^{-5}	$< 2.2\times10^{-16}$
Skew ~ ISL2+C1+C2+YFU	0.7916	-0.0003	3.7457×10^{-5}	$< 2.2\times10^{-16}$
Skew ~ ISL2+C1+C2+YFU+PD	0.7867	-0.0004	3.7453×10^{-5}	$< 2.2\times10^{-16}$
Skew ~ ISL2+C1+C2+YFU+Acc	0.7865	-0.0004	3.7453×10^{-5}	$< 2.2\times10^{-16}$
Skew ~ ISL3+C1+C2	0.8079	-0.0003	3.7460×10^{-5}	$< 2.2\times10^{-16}$
Skew ~ ISL3+C1+C2+Acc	0.7849	-0.0003	3.7456×10^{-5}	$< 2.2\times10^{-16}$
Skew ~ ISL3+C1+C2+pAg	0.7977	-0.0003	3.7457×10^{-5}	$< 2.2\times10^{-16}$
Skew ~ ISL3+C1+C2+PD	0.787	-0.0003	3.7456×10^{-5}	$< 2.2\times10^{-16}$
Skew ~ ISL3+C1+C2+Acc+pAg	0.7862	-0.0004	3.7453×10^{-5}	$< 2.2\times10^{-16}$
Skew ~ ISL3+C1+C2+YFU	0.7905	-0.0003	3.7456×10^{-5}	$< 2.2\times10^{-16}$
Skew ~ ISL3+C1+C2+YFU+PD	0.7857	-0.0004	3.7452×10^{-5}	$< 2.2\times10^{-16}$
Skew ~ ISL3+C1+C2+YFU+Acc	0.7854	-0.0004	3.7453×10^{-5}	$< 2.2\times10^{-16}$
Skew ~ ISL4+C1+C2	0.8085	-0.0003	3.7461×10^{-5}	$< 2.2\times10^{-16}$
Skew ~ ISL4+C1+C2+Acc	0.7829	-0.0003	3.7457×10^{-5}	$< 2.2\times10^{-16}$
Skew ~ ISL4+C1+C2+pAg	0.7982	-0.0003	3.7457×10^{-5}	$< 2.2\times10^{-16}$
Skew ~ ISL4+C1+C2+PD	0.7863	-0.0003	3.7456×10^{-5}	$< 2.2\times10^{-16}$
Skew ~ ISL4+C1+C2+Acc+pAg	0.7846	-0.0004	3.7453×10^{-5}	$< 2.2\times10^{-16}$
Skew ~ ISL4+C1+C2+YFU	0.7903	-0.0003	3.7457×10^{-5}	$< 2.2\times10^{-16}$
Skew ~ ISL4+C1+C2+YFU+PD	0.7851	-0.0004	3.7453×10^{-5}	$< 2.2\times10^{-16}$
Skew ~ ISL4+C1+C2+YFU+Acc	0.7837	-0.0004	3.7453×10^{-5}	$< 2.2\times10^{-16}$

Table S5. Comparison of models explaining the observed distribution of median (Med), maximum body mass (Max) and body mass skewness (Skew). df = degree of freedom; BIC = Bayesian Information Criterion; ΔBIC = difference in BIC with the best model; ω = BIC weight; R^2_{sp}= variance explained by the fixed factor and the spatial autocorrelation combined; R^2_{nsp}= variance explained by the fixed factors only. C1-2 = First two principal components explaining ~ 65% of the variance of environmental variables and order richness; Acc = Accessibility; pAg = Percentage of agricultural areas; PD = Population density; YFU = Year from first land use; ISL = factor to classify cells as islands (ISL1 = <25,000 km^2; ISL2= <100,000 km^2; ISL3 = <500,000 km^2; ISL4 = <750,000,000 km^2).

Model	**df**	**BIC**	**ΔBIC**	**ω**	**R^2_{sp}**	**R^2_{nsp}**
Med ~ C1 + C2 + YFU + Acc	7	-8564.032	0	0.952	0.941	0.082
Med ~ ISL4 + C1 + C2 + YFU + Acc	8	-8557.369	6.662	0.034	0.941	0.086
Med ~ ISL2 + C1 + C2 + YFU + Acc	8	-8555.244	8.787	0.012	0.941	0.083
Med ~ C1 + C2 + Acc	6	-8550.977	13.054	0.001	0.941	0.091
Med ~ C1 + C2 + Acc + pAg	7	-8546.472	17.560	0	0.941	0.086
Med ~ C1 + C2 + YFU + PD	7	-8545.785	18.247	0	0.941	0.062
Med ~ ISL4 + C1 + C2 + Acc	7	-8544.118	19.914	0	0.941	0.096
Med ~ ISL2 + C1 + C2 + Acc	7	-8542.136	21.895	0	0.941	0.093
Med ~ ISL4 + C1 + C2 + Acc + pAg	8	-8540.032	24.000	0	0.941	0.091
Med ~ ISL4 + C1 + C2 + YFU + PD	8	-8539.507	24.525	0	0.941	0.067
Med ~ ISL2 + C1 + C2 + Acc + pAg	8	-8537.844	26.187	0	0.941	0.087
Med ~ ISL2 + C1 + C2 + YFU + PD	8	-8537.146	26.886	0	0.941	0.063
Med ~ C1 + C2 + YFU	6	-8532.794	31.238	0	0.941	0.046
Med ~ C1 + C2 + PD	6	-8527.818	36.213	0	0.941	0.068
Med ~ ISL4 + C1 + C2 + YFU	7	-8526.811	37.221	0	0.941	0.05
Med ~ ISL2 + C1 + C2 + YFU	7	-8524.359	39.672	0	0.941	0.047
Med ~ ISL4 + C1 + C2 + PD	7	-8521.359	42.673	0	0.941	0.074
Med ~ ISL2 + C1 + C2 + PD	7	-8519.137	44.894	0	0.941	0.069
Med ~ C1 + C2 + pAg	6	-8516.601	47.431	0	0.941	0.040
Med ~ ISL4 + C1 + C2 + pAg	7	-8511.129	52.903	0	0.941	0.045

Model	**df**	**BIC**	**ΔBIC**	**ω**	**R^2_{sp}**	**R^2_{nsp}**
Med ~ C1 + C2	5	-8509.927	54.104	0	0.94	0.045
Med ~ ISL2 + C1 + C2 + pAg	7	-8508.521	55.511	0	0.941	0.041
Med ~ ISL4 + C1 + C2	6	-8503.772	60.259	0	0.941	0.049
Med ~ ISL2 + C1 + C2	6	-8501.469	62.563	0	0.941	0.045
Med ~ ISL1 + C1 + C2 + YFU + Acc	8	-8483.757	80.275	0	0.941	0.082
Med ~ ISL1 + C1 + C2 + Acc	7	-8475.722	88.309	0	0.941	0.092
Med ~ ISL3 + C1 + C2 + YFU + Acc	8	-8470.895	93.136	0	0.941	0.082
Med ~ ISL1 + C1 + C2 + Acc + pAg	8	-8467.400	96.632	0	0.941	0.086
Med ~ ISL3 + C1 + C2 + Acc	7	-8463.246	100.785	0	0.941	0.092
Med ~ ISL1 + C1 + C2 + YFU + PD	8	-8460.357	103.675	0	0.941	0.062
Med ~ ISL1 + C1 + C2 + YFU	7	-8456.616	107.415	0	0.941	0.046
Med ~ ISL3 + C1 + C2 + Acc + pAg	8	-8454.669	109.363	0	0.941	0.086
Med ~ ISL3 + C1 + C2 + YFU + PD	8	-8447.793	116.238	0	0.941	0.062
Med ~ ISL1 + C1 + C2 + PD	7	-8446.668	117.363	0	0.941	0.068
Med ~ ISL3 + C1 + C2 + YFU	7	-8444.437	119.594	0	0.941	0.046
Med ~ ISL1 + C1 + C2	6	-8439.581	124.450	0	0.941	0.045
Med ~ ISL1 + C1 + C2 + pAg	7	-8438.970	125.062	0	0.941	0.04
Med ~ ISL3 + C1 + C2 + PD	7	-8434.580	129.452	0	0.941	0.068
Med ~ ISL3 + C1 + C2	6	-8427.942	136.090	0	0.94	0.045
Med ~ ISL3 + C1 + C2 + pAg	7	-8426.588	137.444	0	0.941	0.040
Max ~ ISL4 + C1 + C2 + Acc	7	-17291.362	0	0.943	0.925	0.218
Max ~ ISL4 + C1 + C2 + Acc + pAg	8	-17285.137	6.225	0.042	0.925	0.215
Max ~ ISL4 + C1 + C2 + YFU + Acc	8	-17283.096	8.267	0.015	0.925	0.216
Max ~ ISL2 + C1 + C2 + Acc	7	-17264.127	27.236	0	0.925	0.176
Max ~ ISL2 + C1 + C2 + Acc + pAg	8	-17258.339	33.024	0	0.925	0.173
Max ~ ISL2 + C1 + C2 + YFU + Acc	8	-17256.035	35.328	0	0.925	0.173

Model	**df**	**BIC**	**ΔBIC**	**ω**	**R^2_{sp}**	**R^2_{nsp}**
Max ~ ISL4 + C1 + C2 + PD	7	-17243.395	47.968	0	0.925	0.138
Max ~ ISL4 + C1 + C2 + YFU + PD	8	-17237.463	53.899	0	0.925	0.141
Max ~ ISL4 + C1 + C2 + pAg	7	-17237.179	54.184	0	0.925	0.124
Max ~ ISL4 + C1 + C2	6	-17230.968	60.395	0	0.925	0.105
Max ~ ISL4 + C1 + C2 + YFU	7	-17226.768	64.595	0	0.925	0.113
Max ~ C1 + C2 + Acc	6	-17224.934	66.428	0	0.924	0.173
Max ~ C1 + C2 + Acc + pAg	7	-17220.831	70.532	0	0.924	0.169
Max ~ ISL2 + C1 + C2 + PD	7	-17217.987	73.376	0	0.924	0.099
Max ~ C1 + C2 + YFU + Acc	7	-17217.072	74.290	0	0.924	0.169
Max ~ ISL2 + C1 + C2 + pAg	7	-17212.767	78.595	0	0.924	0.086
Max ~ ISL2 + C1 + C2 + YFU + PD	8	-17212.269	79.094	0	0.924	0.102
Max ~ ISL2 + C1 + C2	6	-17206.012	85.350	0	0.924	0.065
Max ~ ISL2 + C1 + C2 + YFU	7	-17202.041	89.322	0	0.924	0.073
Max ~ C1 + C2 + PD	6	-17181.267	110.095	0	0.924	0.093
Max ~ C1 + C2 + pAg	6	-17179.147	112.216	0	0.924	0.083
Max ~ C1 + C2 + YFU + PD	7	-17175.813	115.550	0	0.924	0.097
Max ~ C1 + C2	5	-17169.744	121.619	0	0.924	0.061
Max ~ C1 + C2 + YFU	6	-17166.060	125.302	0	0.924	0.069
Max ~ ISL3 + C1 + C2 + Acc	7	-16968.042	323.321	0	0.925	0.172
Max ~ ISL3 + C1 + C2 + Acc + pAg	8	-16960.956	330.407	0	0.925	0.170
Max ~ ISL3 + C1 + C2 + YFU + Acc	8	-16959.704	331.658	0	0.925	0.169
Max ~ ISL1 + C1 + C2 + Acc	7	-16930.867	360.496	0	0.925	0.173
Max ~ ISL1 + C1 + C2 + Acc + pAg	8	-16924.547	366.816	0	0.925	0.171
Max ~ ISL1 + C1 + C2 + YFU + Acc	8	-16922.507	368.856	0	0.925	0.170
Max ~ ISL3 + C1 + C2 + PD	7	-16900.981	390.381	0	0.925	0.099
Max ~ ISL3 + C1 + C2 + pAg	7	-16896.481	394.881	0	0.925	0.087
Max ~ ISL3 + C1 + C2 + YFU + PD	8	-16895.813	395.550	0	0.925	0.102

Model	**df**	**BIC**	**ΔBIC**	**ω**	**R^2_{sp}**	**R^2_{nsp}**
Max ~ ISL3 + C1 + C2	6	-16889.228	402.134	0	0.925	0.068
Max ~ ISL3 + C1 + C2 + YFU	7	-16885.710	405.652	0	0.925	0.075
Max ~ ISL1 + C1 + C2 + PD	7	-16864.473	426.890	0	0.924	0.095
Max ~ ISL1 + C1 + C2 + pAg	7	-16861.819	429.544	0	0.924	0.083
Max ~ ISL1 + C1 + C2 + YFU + PD	8	-16859.229	432.134	0	0.924	0.098
Max ~ ISL1 + C1 + C2	6	-16852.920	438.442	0	0.924	0.062
Max ~ ISL1 + C1 + C2 + YFU	7	-16849.294	442.068	0	0.924	0.07
Skew ~ ISL4 + C1 + C2 + YFU + Acc	8	-39027.210	0	0.428	0.906	0.317
Skew ~ ISL4 + C1 + C2 + Acc + pAg	8	-39026.665	0.545	0.326	0.906	0.314
Skew ~ ISL4 + C1 + C2 + Acc	7	-39025.271	1.939	0.162	0.906	0.314
Skew ~ ISL2 + C1 + C2 + YFU + Acc	8	-39022.476	4.734	0.04	0.906	0.311
Skew ~ ISL2 + C1 + C2 + Acc + pAg	8	-39021.693	5.517	0.027	0.906	0.307
Skew ~ ISL2 + C1 + C2 + Acc	7	-39020.751	6.460	0.017	0.906	0.308
Skew ~ ISL4 + C1 + C2 + YFU + PD	8	-39003.944	23.266	0	0.906	0.309
Skew ~ ISL4 + C1 + C2 + pAg	7	-39002.62	24.590	0	0.906	0.303
Skew ~ ISL2 + C1 + C2 + YFU + PD	8	-38998.217	28.993	0	0.906	0.301
Skew ~ ISL4 + C1 + C2 + PD	7	-38997.566	29.644	0	0.906	0.304
Skew ~ ISL2 + C1 + C2 + pAg	7	-38996.541	30.670	0	0.906	0.294
Skew ~ ISL4 + C1 + C2 + YFU	7	-38995.982	31.228	0	0.906	0.305
Skew ~ C1 + C2 + YFU + Acc	7	-38995.865	31.345	0	0.905	0.282
Skew ~ C1 + C2 + Acc	6	-38994.575	32.635	0	0.905	0.28
Skew ~ C1 + C2 + Acc + pAg	7	-38993.117	34.093	0	0.905	0.279
Skew ~ ISL2 + C1 + C2 + PD	7	-38992.041	35.169	0	0.906	0.296
Skew ~ ISL2 + C1 + C2 + YFU	7	-38990.203	37.007	0	0.906	0.297
Skew ~ ISL4 + C1 + C2	6	-38985.954	41.256	0	0.906	0.298
Skew ~ ISL2 + C1 + C2	6	-38980.429	46.781	0	0.906	0.29

Model	**df**	**BIC**	**ΔBIC**	**ω**	**R^2_{sp}**	**R^2_{nsp}**
Skew ~ C1 + C2 + YFU + PD	7	-38971.029	56.181	0	0.906	0.273
Skew ~ C1 + C2 + PD	6	-38965.287	61.923	0	0.906	0.269
Skew ~ C1 + C2 + pAg	6	-38965.246	61.964	0	0.906	0.267
Skew ~ C1 + C2 + YFU	6	-38961.953	65.257	0	0.906	0.270
Skew ~ C1 + C2	5	-38952.542	74.668	0	0.906	0.265
Skew ~ ISL3 + C1 + C2	6	-37803.795	1223.415	0	0.906	0.284
Skew ~ ISL3 + C1 + C2 + Acc	7	-37800.997	1226.213	0	0.906	0.303
Skew ~ ISL3 + C1 + C2 + pAg	7	-37799.445	1227.765	0	0.906	0.288
Skew ~ ISL3 + C1 + C2 + YFU	7	-37798.878	1228.332	0	0.906	0.291
Skew ~ ISL3 + C1 + C2 + PD	7	-37796.019	1231.191	0	0.906	0.29
Skew ~ ISL3 + C1 + C2 + YFU + Acc	8	-37794.495	1232.715	0	0.906	0.305
Skew ~ ISL3 + C1 + C2 + Acc + pAg	8	-37793.919	1233.291	0	0.906	0.301
Skew ~ ISL1 + C1 + C2	6	-37790.854	1236.356	0	0.906	0.279
Skew ~ ISL3 + C1 + C2 + YFU + PD	8	-37790.581	1236.629	0	0.906	0.295
Skew ~ ISL1 + C1 + C2 + Acc	7	-37787.999	1239.211	0	0.906	0.297
Skew ~ ISL1 + C1 + C2 + YFU	7	-37785.861	1241.349	0	0.906	0.286
Skew ~ ISL1 + C1 + C2 + pAg	7	-37785.581	1241.629	0	0.906	0.283
Skew ~ ISL1 + C1 + C2 + PD	7	-37783.385	1243.825	0	0.906	0.285
Skew ~ ISL1 + C1 + C2 + YFU + Acc	8	-37781.445	1245.765	0	0.906	0.299
Skew ~ ISL1 + C1 + C2 + Acc + pAg	8	-37780.278	1246.932	0	0.906	0.296
Skew ~ ISL1 + C1 + C2 + YFU + PD	8	-37777.834	1249.376	0	0.906	0.290

Table S6. Coefficient estimates (SE) for all models. C1-2 = First two principal components explaining ~ 65% of the variance of environmental variables and order richness; Acc = Accessibility; pAg = Percentage of agricultural areas; PD = Population density; YFU = Year from first land use; ISL = factor to classify cells as islands (ISL1 = <25,000 km^2; ISL2= <100,000 km^2; ISL3 = <500,000 km^2; ISL4 = <750,000,000 km^2). P-values: * = <0.05; ** = <0.01; *** = <0.001.

Model	**Int**	**Comp1**	**Comp2**	**Acc**	**pAg**	**PD**	**YFU**	**ISL1**	**ISL2**	**ISL3**	**ISL4**
Med ~ C1 + C2	-0.364 (0.019) ***	0.015 (0.007) *	-0.054 (0.011) ***	-	-	-	-	-	-	-	-
Med ~ C1 + C2 + Acc	-0.356 (0.018) ***	0.013 (0.007)	-0.071 (0.011) ***	0.035 (0.005) ***	-	-	-	-	-	-	-
Med ~ C1 + C2 + pAg	-0.359 (0.019) ***	0.013 (0.007)	-0.057 (0.011) ***	-	-0.014 (0.005) **	-	-	-	-	-	-
Med ~ C1 + C2 + PD	-0.361 (0.019) ***	0.010 (0.007)	-0.061 (0.011) ***	-	-	-0.020 (0.005) ***	-	-	-	-	-
Med ~ C1 + C2 + Acc + pAg	-0.354 (0.019) ***	0.012 (0.007)	-0.071 (0.011) ***	0.034 (0.005) ***	-0.005 (0.005)	-	-	-	-	-	-
Med ~ C1 + C2 + YFU	-0.361 (0.019) ***	0.013 (0.007)	-0.056 (0.011) ***	-	-	-	-0.020 (0.004) ***	-	-	-	-
Med ~ C1 + C2 + YFU + PD	-0.358 (0.019) ***	0.008 (0.007)	-0.062 (0.011) ***	-	-	-0.018 (0.005) ***	-0.019 (0.004) ***	-	-	-	-
Med ~ C1 + C2 + YFU + Acc	-0.354 (0.019) ***	0.011 (0.007)	-0.071 (0.011) ***	0.032 (0.005) ***	-	-	-0.017 (0.004) ***	-	-	-	-

Model	Int	Comp1	Comp2	Acc	pAg	PD	YFU	ISL1	ISL2	ISL3	ISL4
Med ~ ISL1 + C1 + C2	-0.385 (0.020) ***	0.015 (0.007) *	-0.054 (0.011) ***	-	-	-	-	0.065 (0.019) ***	-	-	-
Med ~ ISL1 + C1 + C2 + Acc	-0.377 (0.019) ***	0.012 (0.007)	-0.072 (0.011) ***	0.035 (0.005) ***	-	-	-	0.067 (0.019) ***	-	-	-
Med ~ ISL1 + C1 + C2 + pAg	-0.381 (0.020) ***	0.012 (0.007)	-0.057 (0.011) ***	-	-0.015 (0.005) **	-	-	0.068 (0.019) ***	-	-	-
Med ~ ISL1 + C1 + C2 + PD	-0.383 (0.020) ***	0.010 (0.007)	-0.061 (0.011) ***	-	-	-0.020 (0.005) ***	-	0.066 (0.019) ***	-	-	-
Med ~ ISL1 + C1 + C2 + Acc + pAg	-0.376 (0.020) ***	0.011 (0.007)	-0.072 (0.011) ***	0.034 (0.005) ***	-0.006 (0.005)	-	-	0.068 (0.019) ***	-	-	-
Med ~ ISL1 + C1 + C2 + YFU	-0.383 (0.020) ***	0.012 (0.007)	-0.056 (0.011) ***	-	-	-	-0.020 (0.004) ***	0.067 (0.019) ***	-	-	-
Med ~ ISL1 + C1 + C2 + YFU + PD	-0.381 (0.020) ***	0.008 (0.007)	-0.062 (0.011) ***	-	-	-0.018 (0.005) ***	-0.019 (0.004) ***	0.067 (0.019) ***	-	-	-
Med ~ ISL1 + C1 + C2 + YFU + Acc	-0.376 (0.019) ***	0.010 (0.007)	-0.072 (0.011) ***	0.032 (0.005) ***	-	-	-0.017 (0.004) ***	0.068 (0.019) ***	-	-	-
Med ~ ISL2 + C1 + C2	-0.374 (0.020) ***	0.015 (0.007) *	-0.055 (0.011) ***	-	-	-	-	-	0.026 (0.018)	-	-
Med ~ ISL2 + C1 + C2 + Acc	-0.366 (0.020) ***	0.012 (0.007)	-0.072 (0.011) ***	0.035 (0.005) ***	-	-	-	-	0.026 (0.018)	-	-
Med ~ ISL2 + C1 + C2 + pAg	-0.37 (0.020)	0.012 (0.007)	-0.057 (0.011)	-	-0.015 (0.005)	-	-	-	0.028 (0.018)	-	-

Model	**Int**	**Comp1**	**Comp2**	**Acc**	**pAg**	**PD**	**YFU**	**ISL1**	**ISL2**	**ISL3**	**ISL4**
	***		***		**						
Med ~ ISL2 + C1 + C2 + PD	-0.371 (0.020) ***	0.010 (0.007)	-0.061 (0.011) ***	-	-	-0.020 (0.005) ***	-	-	0.025 (0.018)	-	-
Med ~ ISL2 + C1 + C2 + Acc + pAg	-0.365 (0.020) ***	0.011 (0.007)	-0.072 (0.011) ***	0.033 (0.005) ***	-0.005 (0.005)	-	-	-	0.027 (0.018)	-	-
Med ~ ISL2 + C1 + C2 + YFU	-0.372 (0.020) ***	0.012 (0.007)	-0.057 (0.011) ***	-	-	-	-0.020 (0.004) ***	-	0.027 (0.018)	-	-
Med ~ ISL2 + C1 + C2 + YFU + PD	-0.369 (0.020) ***	0.008 (0.007)	-0.063 (0.011) ***	-	-	-0.018 (0.005) ***	-0.019 (0.004) ***	-	0.027 (0.018)	-	-
Med ~ ISL2 + C1 + C2 + YFU + Acc	-0.365 (0.020) ***	0.010 (0.007)	-0.072 (0.011) ***	0.032 (0.005) ***	-	-	-0.017 (0.004) ***	-	0.028 (0.018)	-	-
Med ~ ISL3 + C1 + C2	-0.370 (0.021) ***	0.015 (0.007) *	-0.054 (0.011) ***	-	-	-	-	-	-	0.015 (0.02)	-
Med ~ ISL3 + C1 + C2 + Acc	-0.362 (0.020) ***	0.013 (0.007)	-0.071 (0.011) ***	0.035 (0.005) ***	-	-	-	-	-	0.016 (0.02)	-
Med ~ ISL3 + C1 + C2 + pAg	-0.367 (0.021) ***	0.012 (0.007)	-0.057 (0.011) ***	-	-0.015 (0.005) **	-	-	-	-	0.018 (0.02)	-
Med ~ ISL3 + C1 + C2 + PD	-0.367 (0.020) ***	0.010 (0.007)	-0.061 (0.011) ***	-	-	-0.020 (0.005) ***	-	-	-	0.014 (0.02)	-
Med ~ ISL3 + C1 + C2 + Acc + pAg	-0.361 (0.020) ***	0.012 (0.007)	-0.072 (0.011) ***	0.034 (0.005) ***	-0.005 (0.005)	-	-	-	-	0.017 (0.02)	-

Model	Int	Comp1	Comp2	Acc	pAg	PD	YFU	ISL1	ISL2	ISL3	ISL4
Med ~ ISL3 + C1 + C2 + YFU	-0.367 (0.021) ***	0.012 (0.007)	-0.056 (0.011) ***	-	-	-	-0.020 (0.004) ***	-	-	0.016 (0.02)	-
Med ~ ISL3 + C1 + C2 + YFU + PD	-0.365 (0.020) ***	0.008 (0.007)	-0.062 (0.011) ***	-	-	-0.018 (0.005) ***	-0.019 (0.004) ***	-	-	0.015 (0.02)	-
Med ~ ISL3 + C1 + C2 + YFU + Acc	-0.361 (0.020) ***	0.011 (0.007)	-0.071 (0.011) ***	0.032 (0.005) ***	-	-	-0.017 (0.004) ***	-	-	0.016 (0.02)	-
Med ~ ISL4 + C1 + C2	-0.377 (0.021) ***	0.015 (0.007) *	-0.055 (0.011) ***	-	-	-	-	-	-	-	0.030 (0.021)
Med ~ ISL4 + C1 + C2 + Acc	-0.369 (0.021) ***	0.013 (0.007)	-0.072 (0.011) ***	0.035 (0.005) ***	-	-	-	-	-	-	0.031 (0.021)
Med ~ ISL4 + C1 + C2 + pAg	-0.374 (0.021) ***	0.012 (0.007)	-0.057 (0.011) ***	-	-0.015 (0.005) **	-	-	-	-	-	0.034 (0.021)
Med ~ ISL4 + C1 + C2 + PD	-0.374 (0.021) ***	0.010 (0.007)	-0.061 (0.011) ***	-	-	-0.020 (0.005) ***	-	-	-	-	0.030 (0.021)
Med ~ ISL4 + C1 + C2 + Acc + pAg	-0.368 (0.021) ***	0.012 (0.007)	-0.072 (0.011) ***	0.033 (0.005) ***	-0.006 (0.005)	-	-	-	-	-	0.033 (0.021)
Med ~ ISL4 + C1 + C2 + YFU	-0.375 (0.021) ***	0.012 (0.007)	-0.057 (0.011) ***	-	-	-	-0.020 (0.004) ***	-	-	-	0.032 (0.021)
Med ~ ISL4 + C1 + C2 + YFU + PD	-0.372 (0.021) ***	0.008 (0.007)	-0.062 (0.011) ***	-	-	-0.018 (0.005) ***	-0.019 (0.004) ***	-	-	-	0.032 (0.021)
Med ~ ISL4 + C1 + C2 + YFU + Acc	-0.368 (0.021)	0.011 (0.007)	-0.072 (0.011)	0.032 (0.005)	-	-	-0.017 (0.004)	-	-	-	0.033 (0.021)

Model	Int	Comp1	Comp2	Acc	pAg	PD	YFU	ISL1	ISL2	ISL3	ISL4
	***		***	***			***				
Max ~ C1 + C2	1.402 (0.014) ***	0.003 (0.005)	0.050 (0.009) ***	-	-	-	-	-	-	-	-
Max ~ C1 + C2 + Acc	1.415 (0.014) ***	0.001 (0.005)	0.036 (0.009) ***	0.036 (0.004) ***	-	-	-	-	-	-	-
Max ~ C1 + C2 + pAg	1.409 (0.014) ***	0.000 (0.006)	0.048 (0.009) ***	-	-0.017 (0.004) ***	-	-	-	-	-	-
Max ~ C1 + C2 + PD	1.408 (0.014) ***	-0.001 (0.006)	0.046 (0.009) ***	-	-	-0.017 (0.004) ***	-	-	-	-	-
Max ~ C1 + C2 + Acc + pAg	1.417 (0.014) ***	0.000 (0.005)	0.036 (0.009) ***	0.034 (0.004) ***	-0.008 (0.004) *	-	-	-	-	-	-
Max ~ C1 + C2 + YFU	1.404 (0.014) ***	0.002 (0.005)	0.049 (0.009) ***	-	-	-	-0.008 (0.003) *	-	-	-	-
Max ~ C1 + C2 + YFU + PD	1.409 (0.014) ***	-0.001 (0.006)	0.045 (0.009) ***	-	-	-0.017 (0.004) ***	-0.007 (0.003) *	-	-	-	-
Max ~ C1 + C2 + YFU + Acc	1.415 (0.014) ***	0.001 (0.005)	0.036 (0.009) ***	0.036 (0.004) ***	-	-	-0.004 (0.003)	-	-	-	-
Max ~ ISL1 + C1 + C2	1.428 (0.014) ***	0.004 (0.005)	0.050 (0.009) ***	-	-	-	-	-0.102 (0.016) ***	-	-	-
Max ~ ISL1 + C1 + C2 + Acc	1.438 (0.014)	0.002 (0.005)	0.037 (0.009)	0.036 (0.004)	-	-	-	-0.103 (0.016)	-	-	-

Model	**Int**	**Comp1**	**Comp2**	**Acc**	**pAg**	**PD**	**YFU**	**ISL1**	**ISL2**	**ISL3**	**ISL4**
	***		***	***				***			
Max ~ ISL1 + C1 + C2 + pAg	1.433 (0.014) ***	0.000 (0.006)	0.048 (0.009) ***	-	-0.016 (0.004) ***	-	-	-0.099 (0.016) ***	-	-	-
Max ~ ISL1 + C1 + C2 + PD	1.433 (0.014) ***	0.000 (0.006)	0.046 (0.009) ***	-	-	-0.017 (0.004) ***	-	-0.102 (0.016) ***	-	-	-
Max ~ ISL1 + C1 + C2 + Acc + pAg	1.440 (0.014) ***	0.000 (0.005)	0.036 (0.009) ***	0.034 (0.004) ***	-0.007 (0.004)	-	-	-0.101 (0.016) ***	-	-	-
Max ~ ISL1 + C1 + C2 + YFU	1.429 (0.014) ***	0.003 (0.005)	0.05 (0.009) ***	-	-	-	-0.007 (0.003) *	-0.101 (0.016) ***	-	-	-
Max ~ ISL1 + C1 + C2 + YFU + PD	1.433 (0.014) ***	-0.001 (0.006)	0.046 (0.009) ***	-	-	-0.017 (0.004) ***	-0.006 (0.003) *	-0.101 (0.016) ***	-	-	-
Max ~ ISL1 + C1 + C2 + YFU + Acc	1.438 (0.014) ***	0.001 (0.005)	0.037 (0.009) ***	0.036 (0.004) ***	-	-	-0.003 (0.003)	-0.102 (0.016) ***	-	-	-
Max ~ ISL2 + C1 + C2	1.429 (0.014) ***	0.004 (0.005)	0.050 (0.009) ***	-	-	-	-	-	-0.094 (0.015) ***	-	-
Max ~ ISL2 + C1 + C2 + Acc	1.439 (0.014) ***	0.002 (0.005)	0.037 (0.009) ***	0.037 (0.004) ***	-	-	-	-	-0.096 (0.015) ***	-	-
Max ~ ISL2 + C1 + C2 + pAg	1.433 (0.014) ***	0.001 (0.006)	0.048 (0.009) ***	-	-0.016 (0.004) ***	-	-	-	-0.092 (0.015) ***	-	-
Max ~ ISL2 + C1 + C2 + PD	1.434 (0.014) ***	0.000 (0.006)	0.046 (0.009) ***	-	-	-0.018 (0.004) ***	-	-	-0.095 (0.015) ***	-	-

Model	**Int**	**Comp1**	**Comp2**	**Acc**	**pAg**	**PD**	**YFU**	**ISL1**	**ISL2**	**ISL3**	**ISL4**
Max ~ ISL2 + C1 + C2 + Acc + pAg	1.440 (0.014) ***	0.000 (0.005)	0.036 (0.009) ***	0.035 (0.004) ***	-0.007 (0.004)	-	-	-	-0.095 (0.015) ***	-	-
Max ~ ISL2 + C1 + C2 + YFU	1.430 (0.014) ***	0.003 (0.005)	0.050 (0.009) ***	-	-	-	-0.007 (0.003) *	-	-0.094 (0.015) ***	-	-
Max ~ ISL2 + C1 + C2 + YFU + PD	1.434 (0.014) ***	-0.001 (0.006)	0.045 (0.009) ***	-	-	-0.017 (0.004) ***	-0.006 (0.003) *	-	-0.095 (0.015) ***	-	-
Max ~ ISL2 + C1 + C2 + YFU + Acc	1.439 (0.014) ***	0.001 (0.005)	0.037 (0.009) ***	0.036 (0.004) ***	-	-	-0.003 (0.003)	-	-0.096 (0.015) ***	-	-
Max ~ ISL3 + C1 + C2	1.445 (0.014) ***	0.003 (0.005)	0.049 (0.009) ***	-	-	-	-	-	-	-0.148 (0.017) ***	-
Max ~ ISL3 + C1 + C2 + Acc	1.454 (0.014) ***	0.001 (0.005)	0.035 (0.009) ***	0.037 (0.004) ***	-	-	-	-	-	-0.149 (0.017) ***	-
Max ~ ISL3 + C1 + C2 + pAg	1.449 (0.014) ***	0.000 (0.006)	0.047 (0.009) ***	-	-0.015 (0.004) ***	-	-	-	-	-0.144 (0.017) ***	-
Max ~ ISL3 + C1 + C2 + PD	1.449 (0.014) ***	-0.001 (0.006)	0.044 (0.009) ***	-	-	-0.018 (0.004) ***	-	-	-	-0.148 (0.017) ***	-
Max ~ ISL3 + C1 + C2 + Acc + pAg	1.455 (0.014) ***	-0.001 (0.005)	0.035 (0.009) ***	0.035 (0.004) ***	-0.006 (0.004)	-	-	-	-	-0.147 (0.017) ***	-
Max ~ ISL3 + C1 + C2 + YFU	1.446 (0.014) ***	0.002 (0.005)	0.048 (0.009) ***	-	-	-	-0.007 (0.003) *	-	-	-0.147 (0.017) ***	-
Max ~ ISL3 + C1 + C2 + YFU + PD	1.450 (0.014)	-0.002 (0.006)	0.044 (0.009)	-	-	-0.017 (0.004)	-0.006 (0.003)	-	-	-0.148 (0.017)	-

Model	**Int**	**Comp1**	**Comp2**	**Acc**	**pAg**	**PD**	**YFU**	**ISL1**	**ISL2**	**ISL3**	**ISL4**
	***		***			***	*			***	
Max ~ ISL3 + C1 + C2 + YFU + Acc	1.454 (0.014) ***	0.000 (0.005)	0.035 (0.009) ***	0.036 (0.004) ***	-	-	-0.003 (0.003)	-	-	-0.148 (0.017) ***	-
Max ~ ISL4 + C1 + C2	1.457 (0.014) ***	0.002 (0.005)	0.049 (0.008) ***	-	-	-	-	-	-	-	-0.181 (0.017) ***
Max ~ ISL4 + C1 + C2 + Acc	1.466 (0.014) ***	0.000 (0.005)	0.035 (0.009) ***	0.037 (0.004) ***	-	-	-	-	-	-	-0.183 (0.017) ***
Max ~ ISL4 + C1 + C2 + pAg	1.461 (0.014) ***	-0.001 (0.005)	0.047 (0.008) ***	-	-0.015 (0.004) ***	-	-	-	-	-	-0.177 (0.017) ***
Max ~ ISL4 + C1 + C2 + PD	1.461 (0.014) ***	-0.002 (0.006)	0.044 (0.009) ***	-	-	-0.018 (0.004) ***	-	-	-	-	-0.181 (0.017) ***
Max ~ ISL4 + C1 + C2 + Acc + pAg	1.467 (0.014) ***	-0.001 (0.005)	0.035 (0.009) ***	0.035 (0.004) ***	-0.006 (0.004)	-	-	-	-	-	-0.181 (0.017) ***
Max ~ ISL4 + C1 + C2 + YFU	1.458 (0.014) ***	0.001 (0.005)	0.049 (0.008) ***	-	-	-	-0.007 (0.003) *	-	-	-	-0.180 (0.017) ***
Max ~ ISL4 + C1 + C2 + YFU + PD	1.462 (0.014) ***	-0.003 (0.006)	0.044 (0.009) ***	-	-	-0.017 (0.004) ***	-0.006 (0.003) *	-	-	-	-0.181 (0.017) ***
Max ~ ISL4 + C1 + C2 + YFU + Acc	1.466 (0.014) ***	0.000 (0.005)	0.035 (0.009) ***	0.036 (0.004) ***	-	-	-0.003 (0.003)	-	-	-	-0.183 (0.017) ***
Skew ~ C1 + C2	0.536 (0.005)	-0.042 (0.002)	-0.018 (0.004)	-	-	-	-	-	-	-	-

Model	**Int**	**Comp1**	**Comp2**	**Acc**	**pAg**	**PD**	**YFU**	**ISL1**	**ISL2**	**ISL3**	**ISL4**
	***	***	***								
Skew ~ C1 + C2 + Acc	0.536 (0.005) ***	-0.042 (0.002) ***	-0.016 (0.004) ***	-0.004 (0.002) *	-	-	-	-	-	-	-
Skew ~ C1 + C2 + pAg	0.535 (0.005) ***	-0.041 (0.002) ***	-0.017 (0.004) ***	-	0.003 (0.002)	-	-	-	-	-	-
Skew ~ C1 + C2 + PD	0.536 (0.005) ***	-0.041 (0.002) ***	-0.017 (0.004) ***	-	-	0.002 (0.002)	-	-	-	-	-
Skew ~ C1 + C2 + Acc + pAg	0.536 (0.005) ***	-0.041 (0.002) ***	-0.016 (0.004) ***	-0.004 (0.002)	0.001 (0.002)	-	-	-	-	-	-
Skew ~ C1 + C2 + YFU	0.536 (0.005) ***	-0.042 (0.002) ***	-0.018 (0.004) ***	-	-	-	0.003 (0.001)	-	-	-	-
Skew ~ C1 + C2 + YFU + PD	0.536 (0.005) ***	-0.041 (0.002) ***	-0.017 (0.004) ***	-	-	0.002 (0.002)	0.003 (0.001)	-	-	-	-
Skew ~ C1 + C2 + YFU + Acc	0.536 (0.005) ***	-0.041 (0.002) ***	-0.016 (0.004) ***	-0.004 (0.002)	-	-	0.002 (0.001)	-	-	-	-
Skew ~ ISL1 + C1 + C2	0.550 (0.005) ***	-0.042 (0.002) ***	-0.017 (0.004) ***	-	-	-	-	-0.074 (0.007) ***	-	-	-
Skew ~ ISL1 + C1 + C2 + Acc	0.550 (0.005) ***	-0.042 (0.002) ***	-0.015 (0.004) ***	-0.005 (0.002) **	-	-	-	-0.075 (0.007) ***	-	-	-
Skew ~ ISL1 + C1 + C2 + pAg	0.550 (0.005) ***	-0.041 (0.002) ***	-0.016 (0.004) ***	-	0.004 (0.002) *	-	-	-0.075 (0.007) ***	-	-	-

Model	**Int**	**Comp1**	**Comp2**	**Acc**	**pAg**	**PD**	**YFU**	**ISL1**	**ISL2**	**ISL3**	**ISL4**
Skew ~ ISL1 + C1 + C2 + PD	0.550 (0.005) ***	-0.041 (0.002) ***	-0.016 (0.004) ***	-	-	0.003 (0.002)	-	-0.074 (0.007) ***	-	-	-
Skew ~ ISL1 + C1 + C2 + Acc + pAg	0.550 (0.005) ***	-0.041 (0.002) ***	-0.014 (0.004) ***	-0.004 (0.002) *	0.003 (0.002)	-	-	-0.075 (0.007) ***	-	-	-
Skew ~ ISL1 + C1 + C2 + YFU	0.550 (0.005) ***	-0.042 (0.002) ***	-0.016 (0.004) ***	-	-	-	0.003 (0.001) *	-0.074 (0.007) ***	-	-	-
Skew ~ ISL1 + C1 + C2 + YFU + PD	0.550 (0.005) ***	-0.041 (0.002) ***	-0.015 (0.004) ***	-	-	0.002 (0.002)	0.003 (0.001) *	-0.075 (0.007) ***	-	-	-
Skew ~ ISL1 + C1 + C2 + YFU + Acc	0.550 (0.005) ***	-0.042 (0.002) ***	-0.014 (0.004) ***	-0.004 (0.002) *	-	-	0.003 (0.001)	-0.075 (0.007) ***	-	-	-
Skew ~ ISL2 + C1 + C2	0.556 (0.005) ***	-0.042 (0.002) ***	-0.016 (0.004) ***	-	-	-	-	-	-0.085 (0.007) ***	-	-
Skew ~ ISL2 + C1 + C2 + Acc	0.556 (0.005) ***	-0.041 (0.002) ***	-0.013 (0.004) ***	-0.005 (0.002) **	-	-	-	-	-0.086 (0.007) ***	-	-
Skew ~ ISL2 + C1 + C2 + pAg	0.556 (0.005) ***	-0.041 (0.002) ***	-0.015 (0.004) ***	-	0.004 (0.002) *	-	-	-	-0.086 (0.007) ***	-	-
Skew ~ ISL2 + C1 + C2 + PD	0.556 (0.005) ***	-0.041 (0.002) ***	-0.015 (0.004) ***	-	-	0.002 (0.002)	-	-	-0.085 (0.007) ***	-	-
Skew ~ ISL2 + C1 + C2 + Acc + pAg	0.556 (0.005) ***	-0.041 (0.002) ***	-0.013 (0.004) ***	-0.004 (0.002) *	0.003 (0.002)	-	-	-	-0.086 (0.007) ***	-	-
Skew ~ ISL2 + C1 + C2 + YFU	0.556 (0.005)	-0.041 (0.002)	-0.015 (0.004)	-	-	-	0.003 (0.001)	-	-0.085 (0.007)	-	-

Model	**Int**	**Comp1**	**Comp2**	**Acc**	**pAg**	**PD**	**YFU**	**ISL1**	**ISL2**	**ISL3**	**ISL4**
	***	***	***				*		***		
Skew ~ ISL2 + C1 + C2 + YFU + PD	0.556 (0.005) ***	-0.041 (0.002) ***	-0.014 (0.004) ***	-	-	0.002 (0.002)	0.003 (0.001) *	-	-0.085 (0.007) ***	-	-
Skew ~ ISL2 + C1 + C2 + YFU + Acc	0.556 (0.005) ***	-0.041 (0.002) ***	-0.013 (0.004) ***	-0.004 (0.002) *	-	-	0.003 (0.001)	-	-0.086 (0.007) ***	-	-
Skew ~ ISL3 + C1 + C2	0.556 (0.005) ***	-0.043 (0.002) ***	-0.016 (0.004) ***	-	-	-	-	-	-	-0.081 (0.007) ***	-
Skew ~ ISL3 + C1 + C2 + Acc	0.557 (0.005) ***	-0.042 (0.002) ***	-0.014 (0.004) ***	-0.005 (0.002) **	-	-	-	-	-	-0.081 (0.007) ***	-
Skew ~ ISL3 + C1 + C2 + pAg	0.556 (0.005) ***	-0.042 (0.002) ***	-0.015 (0.004) ***	-	0.004 (0.002) *	-	-	-	-	-0.082 (0.007) ***	-
Skew ~ ISL3 + C1 + C2 + PD	0.557 (0.005) ***	-0.042 (0.002) ***	-0.015 (0.004) ***	-	-	0.002 (0.002)	-	-	-	-0.081 (0.007) ***	-
Skew ~ ISL3 + C1 + C2 + Acc + pAg	0.557 (0.005) ***	-0.042 (0.002) ***	-0.013 (0.004) ***	-0.004 (0.002) *	0.003 (0.002)	-	-	-	-	-0.082 (0.007) ***	-
Skew ~ ISL3 + C1 + C2 + YFU	0.557 (0.005) ***	-0.042 (0.002) ***	-0.016 (0.004) ***	-	-	-	0.003 (0.001) *	-	-	-0.081 (0.007) ***	-
Skew ~ ISL3 + C1 + C2 + YFU + PD	0.557 (0.005) ***	-0.042 (0.002) ***	-0.015 (0.004) ***	-	-	0.002 (0.002)	0.003 (0.001) *	-	-	-0.081 (0.007) ***	-
Skew ~ ISL3 + C1 + C2 + YFU + Acc	0.557 (0.005) ***	-0.042 (0.002) ***	-0.014 (0.004) ***	-0.004 (0.002) *	-	-	0.003 (0.001)	-	-	-0.081 (0.007) ***	-

Model	Int	Comp1	Comp2	Acc	pAg	PD	YFU	ISL1	ISL2	ISL3	ISL4
Skew ~ ISL4 + C1 + C2	0.561 (0.005) ***	-0.043 (0.002) ***	-0.015 (0.004) ***	-	-	-	-	-	-	-	-0.090 (0.007) ***
Skew ~ ISL4 + C1 + C2 + Acc	0.561 (0.005) ***	-0.043 (0.002) ***	-0.013 (0.004) ***	-0.005 (0.002) **	-	-	-	-	-	-	-0.090 (0.007) ***
Skew ~ ISL4 + C1 + C2 + pAg	0.560 (0.005) ***	-0.042 (0.002) ***	-0.014 (0.004) ***	-	0.004 (0.002) *	-	-	-	-	-	-0.091 (0.007) ***
Skew ~ ISL4 + C1 + C2 + PD	0.561 (0.005) ***	-0.042 (0.002) ***	-0.014 (0.004) ***	-	-	0.003 (0.002)	-	-	-	-	-0.090 (0.007) ***
Skew ~ ISL4 + C1 + C2 + Acc + pAg	0.561 (0.005) ***	-0.042 (0.002) ***	-0.012 (0.004) ***	-0.004 (0.002) *	0.003 (0.002)	-	-	-	-	-	-0.091 (0.007) ***
Skew ~ ISL4 + C1 + C2 + YFU	0.561 (0.005) ***	-0.043 (0.002) ***	-0.015 (0.004) ***	-	-	-	0.003 (0.001) *	-	-	-	-0.090 (0.007) ***
Skew ~ ISL4 + C1 + C2 + YFU + PD	0.561 (0.005) ***	-0.042 (0.002) ***	-0.014 (0.004) ***	-	-	0.002 (0.002)	0.003 (0.001) *	-	-	-	-0.090 (0.007) ***
Skew ~ ISL4 + C1 + C2 + YFU + Acc	0.561 (0.005) ***	-0.042 (0.002) ***	-0.013 (0.004) ***	-0.004 (0.002) *	-	-	0.003 (0.001)	-	-	-	-0.091 (0.007) ***

Table S5. Comparison of models explaining the observed distribution of median (Med), maximum body mass (Max) and body mass skewness (Skew). df = degree of freedom; AIC = Bayesian Information Criterion; ΔAIC = difference in AIC with the best model; ω = AIC weight; R^2_{sp}= variance explained by the fixed factor and the spatial autocorrelation combined; R^2_{nsp}= variance explained by the fixed factors only. C1-2 = First two principal components explaining ~ 65% of the variance of environmental variables and order richness; Acc = Accessibility; pAg = Percentage of agricultural areas; PD = Population density; YFU = Year from first land use; ISL = factor to classify cells as islands (ISL1 = <25,000 km^2; ISL2= <100,000 km^2; ISL3 = <500,000 km^2; ISL4 = <750,000,000 km^2).

Model	**df**	**AIC**	**ΔAIC**	**ω**	**R^2_{sp}**	**R^2_{nsp}**
Med ~ ISL4 + C1 + C2 + YFU + Acc	8	-8618.110	0	0.507	0.941	0.086
Med ~ C1 + C2 + YFU + Acc	7	-8617.18	0.930	0.318	0.941	0.082
Med ~ ISL2 + C1 + C2 + YFU + Acc	8	-8615.985	2.125	0.175	0.941	0.083
Med ~ ISL4 + C1 + C2 + Acc + pAg	8	-8600.773	17.338	0	0.941	0.091
Med ~ ISL4 + C1 + C2 + YFU + PD	8	-8600.248	17.862	0	0.941	0.067
Med ~ C1 + C2 + Acc + pAg	7	-8599.620	18.49	0	0.941	0.086
Med ~ C1 + C2 + YFU + PD	7	-8598.933	19.177	0	0.941	0.062
Med ~ ISL2 + C1 + C2 + Acc + pAg	8	-8598.585	19.525	0	0.941	0.087
Med ~ ISL2 + C1 + C2 + YFU + PD	8	-8597.887	20.223	0	0.941	0.063
Med ~ ISL4 + C1 + C2 + Acc	7	-8597.266	20.844	0	0.941	0.096
Med ~ C1 + C2 + Acc	6	-8596.533	21.577	0	0.941	0.091
Med ~ ISL2 + C1 + C2 + Acc	7	-8595.284	22.826	0	0.941	0.093
Med ~ ISL4 + C1 + C2 + YFU	7	-8579.959	38.151	0	0.941	0.050
Med ~ C1 + C2 + YFU	6	-8578.349	39.761	0	0.941	0.046
Med ~ ISL2 + C1 + C2 + YFU	7	-8577.507	40.603	0	0.941	0.047
Med ~ ISL4 + C1 + C2 + PD	7	-8574.507	43.603	0	0.941	0.074
Med ~ C1 + C2 + PD	6	-8573.374	44.736	0	0.941	0.068
Med ~ ISL2 + C1 + C2 + PD	7	-8572.285	45.825	0	0.941	0.069
Med ~ ISL4 + C1 + C2 + pAg	7	-8564.277	53.833	0	0.941	0.045
Med ~ C1 + C2 + pAg	6	-8562.156	55.954	0	0.941	0.040
Med ~ ISL2 + C1 + C2 + pAg	7	-8561.669	56.441	0	0.941	0.041
Med ~ ISL4 + C1 + C2	6	-8549.328	68.782	0	0.941	0.049

Model	**df**	**AIC**	**ΔAIC**	**ω**	**R^2_{sp}**	**R^2_{nsp}**
Med ~ C1 + C2	5	-8547.890	70.220	0	0.940	0.045
Med ~ ISL2 + C1 + C2	6	-8547.025	71.086	0	0.941	0.045
Med ~ ISL1 + C1 + C2 + YFU + Acc	8	-8544.498	73.612	0	0.941	0.082
Med ~ ISL3 + C1 + C2 + YFU + Acc	8	-8531.636	86.474	0	0.941	0.082
Med ~ ISL1 + C1 + C2 + Acc	7	-8528.870	89.240	0	0.941	0.092
Med ~ ISL1 + C1 + C2 + Acc + pAg	8	-8528.141	89.969	0	0.941	0.086
Med ~ ISL1 + C1 + C2 + YFU + PD	8	-8521.097	97.013	0	0.941	0.062
Med ~ ISL3 + C1 + C2 + Acc	7	-8516.395	101.715	0	0.941	0.092
Med ~ ISL3 + C1 + C2 + Acc + pAg	8	-8515.409	102.701	0	0.941	0.086
Med ~ ISL1 + C1 + C2 + YFU	7	-8509.765	108.345	0	0.941	0.046
Med ~ ISL3 + C1 + C2 + YFU + PD	8	-8508.534	109.576	0	0.941	0.062
Med ~ ISL1 + C1 + C2 + PD	7	-8499.817	118.294	0	0.941	0.068
Med ~ ISL3 + C1 + C2 + YFU	7	-8497.585	120.525	0	0.941	0.046
Med ~ ISL1 + C1 + C2 + pAg	7	-8492.118	125.992	0	0.941	0.040
Med ~ ISL3 + C1 + C2 + PD	7	-8487.728	130.382	0	0.941	0.068
Med ~ ISL1 + C1 + C2	6	-8485.137	132.973	0	0.941	0.045
Med ~ ISL3 + C1 + C2 + pAg	7	-8479.736	138.374	0	0.941	0.040
Med ~ ISL3 + C1 + C2	6	-8473.497	144.613	0	0.940	0.045
Max ~ ISL4 + C1 + C2 + Acc + pAg	8	-17345.600	0	0.534	0.925	0.215
Max ~ ISL4 + C1 + C2 + Acc	7	-17344.267	1.333	0.274	0.925	0.218
Max ~ ISL4 + C1 + C2 + YFU + Acc	8	-17343.558	2.042	0.192	0.925	0.216
Max ~ ISL2 + C1 + C2 + Acc + pAg	8	-17318.801	26.798	0	0.925	0.173
Max ~ ISL2 + C1 + C2 + Acc	7	-17317.031	28.569	0	0.925	0.176
Max ~ ISL2 + C1 + C2 + YFU + Acc	8	-17316.498	29.102	0	0.925	0.173
Max ~ ISL4 + C1 + C2 + YFU + PD	8	-17297.926	47.674	0	0.925	0.141
Max ~ ISL4 + C1 + C2 + PD	7	-17296.300	49.300	0	0.925	0.138
Max ~ ISL4 + C1 + C2 + pAg	7	-17290.083	55.517	0	0.925	0.124
Max ~ ISL4 + C1 + C2	7	-17279.673	65.927	0	0.925	0.113

Model	**df**	**AIC**	**ΔAIC**	**ω**	**R^2_{sp}**	**R^2_{nsp}**
+ YFU						
Max ~ ISL4 + C1 + C2	6	-17276.315	69.285	0	0.925	0.105
Max ~ C1 + C2 + Acc + pAg	7	-17273.736	71.864	0	0.924	0.169
Max ~ ISL2 + C1 + C2 + YFU + PD	8	-17272.731	72.869	0	0.924	0.102
Max ~ ISL2 + C1 + C2 + PD	7	-17270.891	74.709	0	0.924	0.099
Max ~ C1 + C2 + Acc	6	-17270.281	75.319	0	0.924	0.173
Max ~ C1 + C2 + YFU + Acc	7	-17269.977	75.623	0	0.924	0.169
Max ~ ISL2 + C1 + C2 + pAg	7	-17265.672	79.928	0	0.924	0.086
Max ~ ISL2 + C1 + C2 + YFU	7	-17254.945	90.654	0	0.924	0.073
Max ~ ISL2 + C1 + C2	6	-17251.359	94.241	0	0.924	0.065
Max ~ C1 + C2 + YFU + PD	7	-17228.718	116.882	0	0.924	0.097
Max ~ C1 + C2 + PD	6	-17226.614	118.986	0	0.924	0.093
Max ~ C1 + C2 + pAg	6	-17224.494	121.106	0	0.924	0.083
Max ~ C1 + C2 + YFU	6	-17211.407	134.193	0	0.924	0.069
Max ~ C1 + C2	5	-17207.533	138.067	0	0.924	0.061
Max ~ ISL3 + C1 + C2 + Acc + pAg	8	-17021.418	324.182	0	0.925	0.170
Max ~ ISL3 + C1 + C2 + Acc	7	-17020.947	324.653	0	0.925	0.172
Max ~ ISL3 + C1 + C2 + YFU + Acc	8	-17020.167	325.433	0	0.925	0.169
Max ~ ISL1 + C1 + C2 + Acc + pAg	8	-16985.009	360.591	0	0.925	0.171
Max ~ ISL1 + C1 + C2 + Acc	7	-16983.771	361.828	0	0.925	0.173
Max ~ ISL1 + C1 + C2 + YFU + Acc	8	-16982.969	362.631	0	0.925	0.170
Max ~ ISL3 + C1 + C2 + YFU + PD	8	-16956.275	389.325	0	0.925	0.102
Max ~ ISL3 + C1 + C2 + PD	7	-16953.886	391.714	0	0.925	0.099
Max ~ ISL3 + C1 + C2 + pAg	7	-16949.386	396.214	0	0.925	0.087
Max ~ ISL3 + C1 + C2 + YFU	7	-16938.615	406.985	0	0.925	0.075
Max ~ ISL3 + C1 + C2	6	-16934.575	411.025	0	0.925	0.068
Max ~ ISL1 + C1 + C2 + YFU + PD	8	-16919.692	425.908	0	0.924	0.098
Max ~ ISL1 + C1 + C2 + PD	7	-16917.378	428.222	0	0.924	0.095
Max ~ ISL1 + C1 + C2 + pAg	7	-16914.724	430.876	0	0.924	0.083
Max ~ ISL1 + C1 + C2 + YFU	7	-16902.199	443.401	0	0.924	0.070

Model	**df**	**AIC**	**ΔAIC**	**ω**	**R^2_{sp}**	**R^2_{nsp}**
Max ~ ISL1 + C1 + C2	6	-16898.267	447.333	0	0.924	0.062
Skew ~ ISL4 + C1 + C2 + YFU + Acc	8	-39087.951	0	0.519	0.906	0.317
Skew ~ ISL4 + C1 + C2 + Acc + pAg	8	-39087.406	0.545	0.395	0.906	0.314
Skew ~ ISL2 + C1 + C2 + YFU + Acc	8	-39083.217	4.734	0.049	0.906	0.311
Skew ~ ISL2 + C1 + C2 + Acc + pAg	8	-39082.434	5.517	0.033	0.906	0.307
Skew ~ ISL4 + C1 + C2 + Acc	7	-39078.419	9.532	0.004	0.906	0.314
Skew ~ ISL2 + C1 + C2 + Acc	7	-39073.899	14.052	0	0.906	0.308
Skew ~ ISL4 + C1 + C2 + YFU + PD	8	-39064.685	23.266	0	0.906	0.309
Skew ~ ISL2 + C1 + C2 + YFU + PD	8	-39058.958	28.993	0	0.906	0.301
Skew ~ ISL4 + C1 + C2 + pAg	7	-39055.768	32.183	0	0.906	0.303
Skew ~ ISL4 + C1 + C2 + PD	7	-39050.714	37.237	0	0.906	0.304
Skew ~ ISL2 + C1 + C2 + pAg	7	-39049.689	38.262	0	0.906	0.294
Skew ~ ISL4 + C1 + C2 + YFU	7	-39049.130	38.821	0	0.906	0.305
Skew ~ C1 + C2 + YFU + Acc	7	-39049.013	38.938	0	0.905	0.282
Skew ~ C1 + C2 + Acc + pAg	7	-39046.266	41.685	0	0.905	0.279
Skew ~ ISL2 + C1 + C2 + PD	7	-39045.189	42.762	0	0.906	0.296
Skew ~ ISL2 + C1 + C2 + YFU	7	-39043.351	44.600	0	0.906	0.297
Skew ~ C1 + C2 + Acc	6	-39040.131	47.820	0	0.905	0.28
Skew ~ ISL4 + C1 + C2	6	-39031.509	56.442	0	0.906	0.298
Skew ~ ISL2 + C1 + C2	6	-39025.984	61.967	0	0.906	0.29
Skew ~ C1 + C2 + YFU + PD	7	-39024.177	63.774	0	0.906	0.273
Skew ~ C1 + C2 + PD	6	-39010.843	77.108	0	0.906	0.269
Skew ~ C1 + C2 + pAg	6	-39010.802	77.149	0	0.906	0.267
Skew ~ C1 + C2 + YFU	6	-39007.509	80.442	0	0.906	0.270
Skew ~ C1 + C2	5	-38990.505	97.446	0	0.906	0.265
Skew ~ ISL3 + C1 + C2 + YFU + Acc	8	-37855.236	1232.715	0	0.906	0.305
Skew ~ ISL3 + C1 + C2 + Acc + pAg	8	-37854.66	1233.291	0	0.906	0.301
Skew ~ ISL3 + C1 + C2 + Acc	7	-37854.146	1233.805	0	0.906	0.303

Model	**df**	**AIC**	**ΔAIC**	**ω**	**R^2_{sp}**	**R^2_{nsp}**
Skew ~ ISL3 + C1 + C2 + pAg	7	-37852.593	1235.358	0	0.906	0.288
Skew ~ ISL3 + C1 + C2 + YFU	7	-37852.026	1235.925	0	0.906	0.291
Skew ~ ISL3 + C1 + C2 + YFU + PD	8	-37851.322	1236.629	0	0.906	0.295
Skew ~ ISL3 + C1 + C2	6	-37849.351	1238.600	0	0.906	0.284
Skew ~ ISL3 + C1 + C2 + PD	7	-37849.168	1238.783	0	0.906	0.290
Skew ~ ISL1 + C1 + C2 + YFU + Acc	8	-37842.186	1245.765	0	0.906	0.299
Skew ~ ISL1 + C1 + C2 + Acc	7	-37841.148	1246.803	0	0.906	0.297
Skew ~ ISL1 + C1 + C2 + Acc + pAg	8	-37841.019	1246.932	0	0.906	0.296
Skew ~ ISL1 + C1 + C2 + YFU	7	-37839.01	1248.941	0	0.906	0.286
Skew ~ ISL1 + C1 + C2 + pAg	7	-37838.729	1249.222	0	0.906	0.283
Skew ~ ISL1 + C1 + C2 + YFU + PD	8	-37838.575	1249.376	0	0.906	0.290
Skew ~ ISL1 + C1 + C2 + PD	7	-37836.534	1251.417	0	0.906	0.285
Skew ~ ISL1 + C1 + C2	6	-37836.409	1251.542	0	0.906	0.279